

Relaxation of Projected Prior with Continuous Gap Shrinkage

Leo Duan*

Department of Statistics, University of Florida

AND

Sunghyun Cho

Department of Statistics, University of Florida

AND

Mingzhang Yin

Department of Marketing, University of Florida

Abstract

Projected priors were originally introduced to accommodate parameter constraints, but have recently regained popularity due to their ability to assign probability mass to low-dimensional parameter sets, such as the spaces of sparse vectors, directed acyclic graphs, or transport plans. When employed as a transformation of random variables, projection is especially useful, since its contraction property not only preserves probability concentration, but also often preserves differentiability for gradient-based posterior computation. On the other hand, unless the projection can be obtained by some non-iterative algorithm, posterior computation can be expensive because it requires nesting an iterative optimization routine within each Markov chain Monte Carlo iteration. In this article, inspired by the success of continuous shrinkage models as replacements for discrete spike-and-slab priors, we propose a continuous relaxation of projected priors. The key idea is to quantify the duality gap between the primal projection loss and the dual objective, and impose a probabilistic prior that shrinks this gap toward zero. The resulting gap-shrinkage prior has a tractable form, does not require running an optimization subroutine inside each posterior update, and puts probability mass near the exact projection. We demonstrate useful properties of gap-shrinkage priors, including connections to global-local shrinkage priors, broad applicability to generalized projection functions, and competitive performance in posterior contraction. We apply the gap-shrinkage model to a marketing data analysis aimed at identifying important predictor effects on multivariate grocery-shopping decisions.

The implementation source code for the models in this article can be found at <https://github.com/leoduan/gap-shrinkage-model>

Keywords: Proximal mapping, Fenchel-Young gap, Contraction rate, Gibbs sampler, Basket data analysis.

1 Introduction

Modern statistical applications often face problems of structured inference: the parameter of interest is not free to vary over a full Euclidean space, but is instead constrained to lie

*li.duan@ufl.edu

in a set with scientific or geometric meaning. Such a structure arises, for example, when regression functions are shape-restricted, coefficient vectors are sparse, matrices are low rank, or graphs obey combinatorial restrictions. In the Bayesian literature, there are at least three broad ways to encode this information. A classical approach is to place a prior directly on the constrained space, as in constrained-support Bayesian analysis (Gelfand et al., 1992; Dunson and Neelon, 2003; Neelon and Dunson, 2004; Mohammadi and Wit, 2015; Li et al., 2019; Agrell, 2019). A second approach is to relax the constraint by defining prior mass through distance to the target set, thereby replacing a hard support restriction with a continuous neighborhood around the constrained space (Duan et al., 2020; Presman and Xu, 2023). A third approach is to begin with a continuous ambient random variable and map it to the structured set by projection (Lin and Dunson, 2014; Astfalck et al., 2024; Xu and Duan, 2023; Xu et al., 2024; Thompson et al., 2024; Bhaumik et al., 2022; Pal and Ghosal, 2025). These three strategies all aim to respect structure, but they differ sharply in how they distribute prior mass and in the computational burdens they impose.

Projection differs from the other two approaches in a particularly important way: it does not only confine probability mass in the constrained set, but transports positive mass onto or near the lower-dimensional faces of that set, such as its boundary. This feature is often statistically desirable because the boundary frequently contains the most interpretable or parsimonious objects. For the ball generated by the ℓ_1 -norm, for example, boundary points include vectors with exact zeros, so projection naturally yields sparse representations (Duchi et al., 2008). For the nuclear-norm ball, even though the interior contains matrices of all ranks (Fazel et al., 2001), the boundary contains matrices with some singular values equal to zero, hence suitable for low-rank matrix estimation. For the space of joint probability matrix (one with non-negative entries that sum to one), the boundary contains matrices with some entries equal to zero, hence suitable for estimating a parsimonious transport plan between two marginal distributions (Peyré and Cuturi, 2019). This perspective is reflected in the broader proximal-mapping Bayesian approach that harnesses generalized projection for model building and posterior computation (Polson et al., 2015; Xu et al., 2024; Zhou et al., 2024).

The above geometric intuition helps explain the growing appeal of projected priors in Bayesian methodology. Projection onto a closed convex set is non-expansive, so it preserves concentration rather than amplifying uncertainty, and this stability makes projection a natural transformation of a continuous latent variable. In favorable settings, the projection map is differentiable almost surely, which allows one to combine structured priors with gradient-based posterior computation. These ideas have already appeared in several forms in the literature. Lin and Dunson (2014) used Gaussian-process projection to obtain Bayesian monotone regression under shape constraints. Xu and Duan (2023) introduced the ℓ_1 -ball prior, which generates exact zeros via projection. This projection-based approach (and its variation) to inducing sparsity has been applied in various settings, including sparse vector autoregressive models (Hadj-Amar et al., 2024), soft-thresholded Gaussian processes (Kang et al., 2018). Xu et al. (2024) generalized the same philosophy through proximal mappings, covering sparsity, fused structure, low-rank matrices, and other varying-dimensional spaces. Thompson et al. (2024) used projection-induced distributions to define priors supported on sparse directed acyclic graphs. Closely related ideas also appear in the broader literature on structured priors, including sparse Bayesian inverse problems (Everink et al., 2023), image-on-scalar regression (Zeng et al., 2024), and changepoint detection for topological image series (Thomas et al., 2025). Together, these developments suggest that projected priors offer a practical route to combining structural regularization, uncertainty quantification, and gradient-guided posterior computation.

Despite these advantages, the practical usefulness of a projected prior depends critically

on the cost of computing the projection, which is itself typically an optimization problem. When the projection map admits a closed form or is solvable by a non-iterative algorithm, posterior computation can be relatively straightforward. But in many cases, the projection is available only as the solution of a complicated distance-minimization problem, requiring iterative numerical routines at each evaluation. For example, when the set is formed by more than one constraint, such as the matrix space under both sparsity and positive semidefinite constraints, the projection does not have a non-iterative solution. Instead, the standard solution is to rely on alternating projection (Bauschke and Borwein, 1996) or Dykstra’s algorithm (Boyle and Dykstra, 1986), which requires multiple iterations to converge. Although convergence is generally rapid for the calculation of one projection, the computational costs add up quickly because the projection may need to be recomputed once or more in each Markov chain Monte Carlo iteration. In addition to computing the projection, numerical differentiation of the projection map can also be burdensome. Automatic differentiation through iterative solution, known as unrolled differentiation, is possible, but comes with a high computational cost unless the number of optimization iterations is small (Scieur et al., 2022).

This challenge is similar to Bayesian variable selection, where exact approaches like spike-and-slab priors yield sparsity but are computationally demanding, leading to the popularity of continuous shrinkage priors as efficient alternatives (Park and Casella, 2008; Carvalho et al., 2009; Polson and Scott, 2011). Likewise, exact projected priors put mass on structured subsets but can be costly to compute. This motivates relaxing exact projection to a continuous prior that strongly favors points near the projection. We pursue this idea through shrinking the primal-dual gap associated with the projection problem. The duality gap is nonnegative and vanishes exactly at the true projection, so it provides a natural relaxation variable: small gap corresponds to near-projection, while zero gap recovers the original projected prior. Importantly, the dual form of the projection constraints often admits a closed-form expression, allowing the duality gap to be computed without iterative optimization.

2 Method

2.1 Constrained set, projection, and duality

To motivate our framework, we first consider a model with likelihood function $\mathcal{L}(y; \theta)$, where y denotes the observed data and $\theta \in \mathbb{R}^p$ is the parameter of interest. Suppose there is a subset $\mathcal{M} \subset \mathbb{R}^p$, representing the set of parameter values that are desirable for purposes of inference, prediction, or interpretation.

Typically, a constrained prior places positive probability only to points within \mathcal{M} and zero probability to points outside \mathcal{M} . Here, we consider those constrained priors that assign positive probability for some constraints to become active (binding in the form of equality). To be illustrative, we start with the classic example of the regression variable selection problem, which ultimately inspires our solution. In variable selection, the constrained space \mathcal{M} can be expressed as

$$\mathcal{M} = \bigcup_{S \subseteq [p]} \{\theta : \theta_j = 0 \ \forall j \in S, \ \theta_k \neq 0 \ \forall k \in [p] \setminus S\},$$

where $[p] = \{1, 2, \dots, p\}$. The union is the \mathbb{R}^p itself, however, positive prior probability is assigned to every subset on the right-hand side of the union, hence $\theta_j = 0 \ \forall j \in S$ become active with a positive probability for some set S . If one assigns a binomial prior probability for each set, then the resulting prior is the discrete spike-and-slab prior.

For general problems, it is challenging to construct priors on sets with active constraints, but projection gives a viable solution. Suppose the subsets of \mathcal{M} lie on the boundary of another set C . We may first draw β from a continuous distribution such as a multivariate Gaussian, and then transform it into θ as the minimizer of a Euclidean distance:

$$\arg \min_{z \in C} \frac{1}{2} \|\beta - z\|_2^2 = \arg \min_z \frac{1}{2} \|\beta - z\|_2^2 + I_C(z), \quad (1)$$

which produces a Euclidean projection $\theta \in \mathcal{M}$ under suitable values of β , and $I_C(\theta)$ is the indicator function that takes value 0 if $\theta \in C$ and $+\infty$ otherwise. It has been well established that when C is a ball based on the ℓ_1 norm $\sum_{j=1}^p |\theta_j|$, or some variant such as $\sum_{g=1}^G \sqrt{\sum_{j \in J_g} \theta_j^2}$, the projection does put positive probability mass on the actively constrained subsets of \mathcal{M} .

Generally, a canonical projected prior approach can be formulated as:

$$\beta \sim \pi_0^\beta(\cdot), \quad \theta = T(\beta), \quad (2)$$

where π_0^β is a base prior distribution on the auxiliary variable β and $T(\beta)$ is the projection of β onto C . The transformation T serves as a change of variables that produces a pushed-forward measure $T_\# \pi_0^\beta$ on θ , which we refer to as the *projected prior*. Equation (2) defines a distribution over the parameter of interest θ by deterministically transforming variable β , a flexible approach for constructing distributions without requiring an explicit density. Specifically, we take the transformation $T(\beta)$ to be the solution to an optimization problem parameterized by β . The Euclidean projection (1) is a special case, and we discuss other forms of T later.

The challenge in adopting the projection prior is that the projection T may not be a tractable optimization solution, meaning that it is not solvable in closed form or by a non-iterative algorithm. Therefore, we first consider the dual form of the projection and quantify the exact projection via the dual gap. Since $I_C(z) = \sup_{u \in \mathbb{R}^p} (u^\top z - \sigma_C(u))$ with $\sigma_C(u) = \sup_{w \in C} u^\top w$ known as the support function of C , we have the following lower bound of projection loss using the max-min inequality,

$$\begin{aligned} \frac{1}{2} \|\beta - z\|_2^2 + I_C(z) &\geq \min_{z \in \mathbb{R}^p} \frac{1}{2} \|\beta - z\|_2^2 + I_C(z) \\ &\geq \sup_{u \in \mathbb{R}^p} \inf_{z \in \mathbb{R}^p} \frac{1}{2} \|\beta - z\|_2^2 + u^\top z - \sigma_C(u) \\ &\geq \beta^\top u - \frac{1}{2} \|u\|^2 - \sigma_C(u). \end{aligned} \quad (3)$$

The rightmost of the inequality is known as the dual function of $u \in \mathbb{R}^p$, given β ; accordingly, the leftmost is known as the primal function of $z \in \mathbb{R}^p$, given β .

The above is commonly known as weak duality, and it holds for any pair of values $(z, u) \in \mathbb{R}^p \times \mathbb{R}^p$, regardless of whether C is convex. Suppose we do not have a tractable solution for the projection problem, but somehow encounter a pair (\hat{z}, \hat{u}) such that $(1/2)\|\beta - \hat{z}\|^2 + I_C(\hat{z}) = \beta^\top \hat{u} - (1/2)\|\hat{u}\|^2 - \sigma_C(\hat{u})$ exactly and the common value is finite. Then every inequality must turn into an equality, and hence \hat{z} is the exact projection. Therefore, the difference between the primal and dual functions, known as the *duality gap*, can be leveraged to characterize the closeness of \hat{z} to the projection.

In Equation (3), even though \hat{u} may seem redundant for our purpose, it computes the dual function as the lower bound and *certifies* the optimality of \hat{z} . In optimization, there are algorithms, namely primal-dual methods, that do not operate directly by minimizing only the primal function, but instead simultaneously update z and u to reduce the duality gap. This motivates us to take a similar approach in Bayesian prior specification by encouraging a small difference between the primal and dual functions.

2.2 Gap-shrinkage prior

We consider a general projection problem of the form

$$\theta = T(\beta) = \arg \min_{z \in C} f(z; \beta)$$

where $\beta \sim \pi_0^\beta(\cdot)$, and we assume the minimizer is unique for almost every β . The family of transformations T include Euclidean projections, proximal mappings, and Bregman projections.

We call f the primal loss function and assume it has an associated minorant function ϕ , hence a dual function d :

$$\begin{aligned} f(z; \beta) &= \sup_{u \in \mathcal{U}} \phi(z, u; \beta), \quad z \in C, \\ d(u; \beta) &= \inf_{z \in C} \phi(z, u; \beta), \quad u \in \mathcal{U}, \end{aligned}$$

in which taking the infimum often yields a dependent relationship among u , z , and β .

The choice of ϕ is not unique, and depends on the optimization technique being used, such as variable splitting, Lagrange multipliers, or Fenchel conjugacy. We discuss the choice of ϕ in more detail in a later section. Regardless, a practical goal is to make d tractable, which in turn yields a tractable gap function

$$f(z; \beta) - d(u; \beta),$$

as an upper bound on $f(z; \beta) - \min_{z \in C} f(z; \beta)$.

Exponentiating the negative of the gap function, we obtain a shrinkage prior:

$$\Pi_0(\theta, u, \beta) \propto \exp[-\alpha \{f(\theta; \beta) - d(u; \beta)\}] \pi_0^\beta(\beta), \quad (4)$$

where $\theta \in C$ and $u \in \mathcal{U}$. We refer to (4) as the *gap-shrinkage prior*, and $\alpha > 0$ is a fixed hyperparameter that controls the strength of the shrinkage effect. Since the duality gap is always non-negative, given (u, β) , the gap-shrinkage prior places high density close to the exact projection where the gap equals zero.

Remark 1. For clarification, note that (u, z) can be chosen to be independent or dependent in the prior specification, and it affects neither the weak duality nor the certification of the optimality of \hat{z} . In several cases presented in the article, we may choose u as some deterministic transform of β and z .

Beyond the Euclidean projection (1), we now focus on a generalized projection known as a proximal mapping, which is the minimizer of the following proximal loss:

$$f(z; \beta) = \frac{1}{2} \|\beta - z\|_2^2 + g(z), \quad (5)$$

where g is a convex and lower semi-continuous function. The minimizer $\arg \min_z f(z; \beta)$ is the proximal mapping, denoted by $\text{prox}_g(\beta)$. The above loss includes the Euclidean projection loss as a special case when $g(z) = I_C(z)$, although more often one uses a penalty form of g instead of $I_C(z)$. Specifically, for Euclidean projection onto the set $C = \{z : h_j(z) \leq r_j, j = 1, \dots, d\}$, where each $h_j : \mathbb{R}^p \mapsto \mathbb{R}$ is convex, one can show that for every (r_1, \dots, r_d) the Euclidean projection is also the minimizer of a proximal loss with penalty function $g(z) = \sum \lambda_j h_j(z)$ for suitable $\lambda_j \geq 0$. The preference for the penalty form over $I_C(z)$ is often driven by its greater computational simplicity.

We first illustrate the gap-shrinkage prior with a simple ℓ_1 -norm proximal mapping.

Example 1. Consider the ℓ_1 -norm proximal loss commonly used for inducing sparsity:

$$f(z; \beta, \lambda) = \frac{1}{2} \|z - \beta\|_2^2 + \lambda \|z\|_1,$$

with $\lambda \geq 0$. In fact, the primal form has a closed-form minimizer $\hat{z} = \text{sign}(\beta)(|\beta| - \lambda)_+$, which was used in the construction of ℓ_1 -ball prior (Xu and Duan, 2023) and soft-thresholded Gaussian process prior (Kang et al., 2018). Nevertheless, interesting continuous priors can be derived via the gap-shrinkage route.

Using the dual norm of ℓ_1 -norm, we can see $\lambda \|z\|_1 = \max_{\|u\|_\infty \leq \lambda} u^\top z$, leading to minorant $\phi(z, u; \beta) = (1/2) \|z - \beta\|_2^2 + u^\top z$. Minimizing over z yields a deterministic relationship $\hat{z} = \beta - u$, and the dual function:

$$d(u; \beta, \lambda) = u^\top \beta - \frac{1}{2} \|u\|^2, \quad \|u\|_\infty \leq \lambda.$$

Setting $\theta = \hat{z}$ as the minimizer and applying $\beta = \theta + u$ to simplify the expression, we have the gap function:

$$f(\hat{z}; \beta) - d(u; \beta) = \lambda \|\theta\|_1 - u^\top \theta$$

We note that each element in the gap $\lambda|\theta_j| - u_j\theta_j$ is smaller when $u_j\theta_j > 0$ than when $u_j\theta_j < 0$; hence we can further impose constraint $u_j\theta_j > 0$ for all $j = 1, \dots, p$. Assigning a Cauchy kernel as the base prior $\pi_0^\beta(\beta)$, we have the following simplified gap-shrinkage prior:

$$\Pi_0(\theta, u \mid \lambda) \propto \exp \left\{ -\alpha \sum_{j=1}^p (\lambda - |u_j|) |\theta_j| \right\} 1(\|u\|_\infty \leq \lambda) \prod_{j=1}^p \{1 + (\theta_j + u_j)^2\}^{-1}.$$

We can see some resemblance to the Bayesian lasso prior $\propto \exp(-\alpha \lambda \|\theta\|_1)$, but also a clear difference in the $\alpha |u_j| |\theta_j|$ term. Effectively, a large α makes the following happen with high probability:

$$(\lambda - |u_j|) |\theta_j| \approx 0 \quad \Leftrightarrow \quad \theta_j \approx 0 \text{ or } \lambda \approx |u_j|.$$

We can immediately see a connection to the global-local shrinkage literature (Polson and Scott, 2011): $\lambda \gg |u_j|$ leads to a strong global shrinkage effect driving θ_j toward the zero (active constraint), while the dual parameter u_j provides a local adjustment allowing θ_j to escape from zero as $|u_j| \uparrow \lambda$.

Remark 2. In the supplementary material, we prove that under Cauchy kernel for π_0^β , the marginal prior $\pi_0(\theta_j \mid \lambda)$ has a power-law tail, instead of exponential decay as in the Bayesian lasso prior. ■

For generalized ℓ_1 -norm proximal losses of the form $g(z) = \lambda \|Dz\|_1$, the primal loss function does not have a tractable solution. Yet such losses have important applications in graph-based smoothing, change-point detection, and other structured sparsity problems. For example, if a list of contrasts $(i, j) \in E$ is represented as edges in a graph $G = ([p], E)$, then D can be taken as the corresponding contrast design matrix with values in $\{-1, 0, 1\}^{|E| \times p}$. We now derive the associated gap-shrinkage prior.

Example 2. Consider the proximal loss $f(z; \beta, \lambda) = \frac{1}{2} \|z - \beta\|_2^2 + \lambda \|Dz\|_1$, for $D \in \mathbb{R}^{d \times p}$. Using a variable splitting technique $Dz = w$ and Lagrangian multiplier $u \in \mathbb{R}^d$, we have

$$\phi(z, w, u; \beta) = \frac{1}{2} \|z - \beta\|_2^2 + \lambda \|w\|_1 + u^\top (Dz - w).$$

Minimizing over z and w yields relationship $\theta = \hat{z} = \beta - D^\top u$ and $\min_w \lambda \|w\|_1 - u^\top w = 0$ if $\|u\|_\infty \leq \lambda$ (otherwise, the infimum is $-\infty$), hence the dual function is:

$$d(u; \beta, \lambda) = -\frac{1}{2} \|D^\top u\|_2^2 + \beta^\top D^\top u, \quad \|u\|_\infty \leq \lambda.$$

Using a similar constraint $u_j (D\theta)_j > 0$ and assigning a Cauchy kernel π_0^β , replacing z in primal loss function with the minimum θ , we have a gap-shrinkage prior:

$$\Pi_0(\theta, u \mid \lambda) \propto \exp \left\{ -\alpha \sum_{j=1}^d (\lambda - |u_j|) |(D\theta)_j| \right\} \mathbf{1}(\|u\|_\infty \leq \lambda) \prod_{j=1}^p \{1 + (\theta_j + D_j^\top u)^2\}^{-1}.$$

Note a similar adaptive shrinkage effect on $D\theta$ as in the last example. ■

2.3 Properties of gap-shrinkage

We now derive some useful properties of gap-shrinkage priors. We first generalize the examples above to broad proximal mapping projection (5).

2.3.1 Tractable relaxation of proximal mapping projection

Our goal is to derive a tractable form of the gap-shrinkage prior for proximal mapping (5), so that readers can readily apply it to their choice of g . Using variable splitting $z = w$, we have the Lagrangian for (5):

$$\phi(z, w, u; \beta) = \frac{1}{2} \|\beta - z\|^2 + g(w) + u^\top (z - w),$$

whose minimization over (z, w) yields $z = \beta - u$, $u \in \mathbb{R}^p$, and the dual function:

$$d(u; \beta) = u^\top \beta - \frac{1}{2} \|u\|^2 - g^*(u),$$

where $g^*(u) = \sup_w \{u^\top w - g(w)\}$ is known as the Fenchel conjugate of g .

Therefore, we have the gap function under $z = \beta - u$:

$$\begin{aligned} f(z; \beta) - d(u; \beta) &= \frac{1}{2} \|\beta - z\|^2 + g(z) - u^\top \beta + \frac{1}{2} \|u\|^2 + g^*(u) \\ &= g^*(u) + g(z) - u^\top z \Big|_{z=\beta-u}. \end{aligned} \tag{6}$$

We already know the non-negativity of the left hand side. In the meantime, the non-negativity of the right hand side is also famously known as the Fenchel–Young inequality, and trivially provable using the definition $g^*(u)$ as a supremum.

As a result, the gap-shrinkage prior for proximal mapping is given by

$$\Pi_0(\theta, u \mid \lambda) \propto \exp [-\alpha \{g^*(u) + g(\theta) - u^\top \theta\}] \pi_0^\beta(\theta + u),$$

where we replace z in the primal function with the minimizer θ and apply $\theta = z = \beta - u$ (i.e., $\beta = \theta + u$) in π_0^β . In practice, many Fenchel conjugates admit closed-form expressions. Here are a few common examples. For $g(z) = \|z\|$ with respect to some norm $\|\cdot\|$, the conjugate is $g^*(u) = I_{\{v: \|v\|_* \leq 1\}}(u)$, with $\|\cdot\|_*$ denoting the dual norm. When $g(z) = \frac{1}{2} z^\top Q z$ for a positive definite Q , the conjugate becomes $g^*(u) = \frac{1}{2} u^\top Q^{-1} u$. We note that the gap function in Examples 1 and 2 can be derived from (6) as well.

2.3.2 Effectiveness of shrinkage

Next, we establish the effectiveness of shrinkage. Specifically, since $T(\beta)$ is intractable and we can only quantify $f(z; \beta) - d(u; \beta)$, how far is the relaxed z from the exact $T(\beta)$? We can now use the following theorem to quantify the difference.

Theorem 1. *If $f(z; \beta)$ is μ -strongly convex, i.e., $f(z; \beta) - (\mu/2)\|z\|_2^2$ is convex, its unique minimizer $\hat{z} = \arg \min_z f(z; \beta)$, then for any $z \in C$ and $u \in \mathcal{U}$,*

$$\|z - \hat{z}\|_2 \leq \sqrt{\frac{2}{\mu} \{f(z; \beta) - d(u; \beta)\}}.$$

The proof is based on a direct application of strong convexity. The theorem reveals that encouraging a small duality gap effectively bounds the deviation of the relaxed z from the exact $T(\beta)$. For example, we can immediately see that proximal mapping (including Euclidean projection to convex set as a special case) with a convex g is 1-strongly convex, hence

$$\|z - T(\beta)\|_2 \leq \sqrt{2\{f(z; \beta) - d(u; \beta)\}}.$$

To obtain more general results applicable to a broad class of projections, we introduce the Bregman projection, which minimizes the *Bregman divergence*:

$$D_\psi(z, \beta) = \psi(z) - \psi(\beta) - (z - \beta)^\top \nabla \psi(\beta), \quad (7)$$

with $\psi : \mathbb{R}^p \rightarrow \mathbb{R} \cup \{+\infty\}$ an extended-value function that is continuously differentiable, strictly convex. We can obtain Bregman projection as

$$T(\beta) = \arg \min_{z \in \mathbb{R}^p} D_\psi(z, \beta) + I_C(z).$$

The Bregman divergence D_ψ is a generalization of the squared Euclidean distance, which is a special case when $\psi(z) = \|z\|_2^2$. The Bregman divergence D_ψ may be asymmetric and need not satisfy the triangle inequality, but it provides a natural notion of discrepancy tailored to the geometry induced by ψ , and includes popular measures such as Kullback–Leibler (KL) divergence.

If ψ is further μ -strongly convex, then we know the bound in Theorem 1 applies on $\|z - T(\beta)\|_2$. On the other hand, strong convexity is not necessary if we want to have effective control on the Bregman divergence between z and $T(\beta)$, as shown in the following theorem.

Theorem 2. *If D_ψ is a Bregman divergence generated by a continuously differentiable, strictly convex function $\psi : \mathbb{R}^p \rightarrow \mathbb{R} \cup \{+\infty\}$, then for the primal $f(z; \beta) = D_\psi(z, \beta) + I_C(z)$, the dual function is*

$$d(u; \beta) = -\psi^*(\nabla \psi(\beta) - u) - \sigma_C(u) + \beta^\top \nabla \psi(\beta) - \psi(\beta),$$

with $u \in \mathbb{R}^p$. Let the unique minimizer be $\hat{z} = \arg \min_z D_\psi(z, \beta) + I_C(z)$. Then, for any $z \in C$ and $u \in \mathbb{R}^p$,

$$D_\psi(z, \hat{z}) \leq f(z; \beta) - d(u; \beta).$$

Note that the theorem applies to ψ with domain \mathbb{R}^p . For those $D_{\tilde{\psi}}$ generated by $\tilde{\psi}$ with domain $\Omega \subseteq \mathbb{R}^p$, one could use $\psi(z) = \tilde{\psi}(z) + I_\Omega(z)$ to reconcile the domain difference, provided the divergence is calculated for points where the gradient exists.

We now illustrate the Bregman projection and the gap function.

Example 3. A canonical example is negative entropy $\psi(z) = \sum_{j=1}^p z_j \log z_j + I_{\Delta^{p-1}}(z)$ for $z \in \mathbb{R}^p$, whose associated Bregman divergence is KL divergence $D_\psi(z, \beta) = \sum_{j=1}^p z_j \log(z_j/\beta_j)$. Let $C_0 \subset \mathbb{R}^p$ be a convex set and let $\Delta^{p-1} = \{z : z \geq 0, \sum_{j=1}^p z_j = 1\}$ denote the probability simplex (which is convex). If z lies in $C_0 \cap \Delta^{p-1}$, then we see the Bregman projection gives the KL projection from $\beta \in \Delta^{p-1}$ to a subset:

$$T(\beta) = \arg \min_{z \in C_0 \cap \Delta^{p-1}} \sum_{j=1}^p z_j \log \frac{z_j}{\beta_j}.$$

Compared to the Euclidean projection that could produce $z_j = 0$, we note that the above projection preserves positivity, which is often more natural for probability parameters. Since for $\psi(z) = \sum_{j=1}^p z_j \log z_j + I_{\Delta^{p-1}}(z)$, the Fenchel conjugate is $\psi^*(u) = \log \left(\sum_{j=1}^p e^{u_j} \right)$. We derive the dual function explicitly: $d(u; \beta) = -\log \left(\sum_{j=1}^p \beta_j e^{-u_j} \right) - \sigma_{C_0}(u)$, where $\sigma_{C_0}(u) = \sup_{z \in C_0} \langle u, z \rangle$ is the support function of C_0 . Therefore, the gap function takes the form

$$\sum_{j=1}^p z_j \log \frac{z_j}{\beta_j} + \log \left(\sum_{j=1}^p \beta_j e^{-u_j} \right) + \sigma_{C_0}(u).$$

■

2.4 Variational gap function for complicated settings

In complex settings, the gap function may be either not fully tractable or computationally expensive to evaluate. In this section, we discuss how to handle these cases by introducing a variational gap function:

$$\tilde{G}(z, v; \beta) \geq f(z; \beta) - d(u; \beta), \quad \text{for all } z, u, v,$$

and $\exists v = v(z, u, \beta)$ such that the equality can be achieved for any (z, u) . Therefore, we see the variational gap function is a tight upper bound of the true gap function, hence allowing us to use $\exp[-\alpha \tilde{G}(\theta, v; \beta)]$ for gap-shrinkage.

To be more concrete, we now discuss two applications of the variational gap function. In the first case, in proximal mappings, it is common to have an additive $g(z) = \sum_{j=1}^J g_j(z)$, such as a sum of different regularizers or cost functions, where each g_j has a tractable Fenchel conjugate. To handle this complication, we can use the Fenchel conjugate for the additive functions given by infimum convolution:

$$g(z) = \sum_{j=1}^J g_j(z) \quad \text{then} \quad g^*(u) = \inf_{\sum_{j=1}^J v_j = u} \sum_{j=1}^J g_j^*(v_j). \quad (8)$$

We see that the infimum convolution may not have a closed-form solution. Instead, we can use a variational gap function:

$$\tilde{G}(z, v; \beta) = \sum_{j=1}^J g_j^*(v_j) + g(z) - \sum_{j=1}^J v_j^\top z \Big|_{z = \beta - \sum_{j=1}^J v_j}, \quad (9)$$

corresponding to $v = (v_1, \dots, v_J)$, each $v_j \in \mathbb{R}^p$; $\tilde{G}(z, v; \beta)$ is a reachable upper bound of the duality gap because $\sum_{j=1}^J g_j^*(v_j) \geq g^*(u)$ by (8), which can then be plugged into the gap function in Equation (6).

Example 4. Consider the projection to a set $C = \bigcap_{j=1}^J C_j$, with each C_j a convex set. Using $g_j(z) = I_{C_j}(z)$, we can see that $g(z) = \sum_{j=1}^J I_{C_j}(z)$ is equivalent to $I_C(z)$. Therefore, the additive form of g corresponds to the projection to the intersection of the sets. Since $I_{C_j}(z)$ has Fenchel conjugate $\sigma_{C_j}(v_j)$, the support function of C_j , we have the gap-shrinkage prior given by

$$\Pi_0(\theta, v_1, \dots, v_J \mid \lambda) \propto \exp \left[-\alpha \sum_{j=1}^J \{ \sigma_{C_j}(v_j) - v_j^\top \theta \} \right] \pi_0^\beta(\theta + \sum_{j=1}^J v_j) \mathbf{1}(\theta \in C_j).$$

For simple convex sets C_j , the support function $\sigma_{C_j}(v_j)$ has a closed-form expression. For example, for a ball $C_j = \{z : \|z\| \leq r\}$, generated by some norm $\|\cdot\|$, we have $\sigma_{C_j}(v_j) = r \|v_j\|_*$.

For a concrete application, for group-wise sparsity, we may consider a projected prior generated by the intersection of the sets $C_j = \{z : \sqrt{\sum_{i \in G_j} z_i^2} \leq r_j\}$, where G_j is a group of indices that we want the elements of θ_j to be simultaneously zero or non-zero. The associated support function is $\sigma_{C_j}(u_j) = r_j \sqrt{\sum_{i \in G_j} u_{j,i}^2}$, since the dual norm of the ℓ_2 norm is another ℓ_2 norm. ■

The second application involves a matrix-valued parameter $\theta \in \mathbb{R}^{p_1 \times p_2}$, whose operations may be expensive. For example, for projection to a low-rank space, one often needs to apply some matrix decomposition such as singular value decomposition (SVD), which is cubic order of $O(p_1 p_2 \min(p_1, p_2))$. This motivates us to develop a variational gap function.

Example 5. Let $\theta \in \mathbb{R}^{p_1 \times p_2}$ be a matrix parameter and take $g(\theta) = \lambda \|\theta\|_*$, where $\|\cdot\|_*$ denotes the nuclear norm, the sum of the singular values of θ . The Fenchel conjugate of g is the indicator of the operator-norm ball, $g^*(u) = I_{\{\|u\|_{\text{op}} \leq \lambda\}}(u)$, with $u \in \mathbb{R}^{p_1 \times p_2}$. Substituting into (6) gives the gap

$$f(z; \beta) - d(u; \beta) = \lambda \|\theta\|_* - \langle u, \theta \rangle, \quad \|u\|_{\text{op}} \leq \lambda, \quad \theta = \beta - u.$$

The proximal mapping with respect to this g has a closed-form solution given by singular-value soft-thresholding of θ , but this approach requires computing the SVD of θ . The same burden applies to evaluating $\|\theta\|_*$. Instead, we use the variational form:

$$\|\theta\|_* = \min_{\substack{A \in \mathbb{R}^{p_1 \times r}, B \in \mathbb{R}^{p_2 \times r} \\ AB^\top = \theta}} \frac{1}{2} (\|A\|_F^2 + \|B\|_F^2),$$

which holds for any $r = \min(p_1, p_2)$. After reparameterizing, we have a modified gap-shrinkage prior given by

$$\Pi_0(\theta = AB^\top, u \mid \lambda) \propto \exp \left[-\alpha \left\{ \frac{\lambda}{2} (\|A\|_F^2 + \|B\|_F^2) - \langle u, AB^\top \rangle \right\} \right] \pi_0^\beta(AB^\top + u),$$

where $\|u\|_{\text{op}} \leq \lambda$. The norm constraint can be enforced via $u = \kappa w / \|w\|_{\text{op}}$, with $\kappa \in (0, \lambda)$, and $\|w\|_{\text{op}}$ the operator norm of w estimated via power iteration. ■

2.5 Posterior under gap-shrinkage

We denote the likelihood as $\mathcal{L}(y; \theta, \kappa)$ with y the data and κ some other parameters (such as λ used above) associated with a prior $\Pi_0(\kappa)$, then our posterior is given by

$$\Pi(\theta, u, \kappa \mid y) = \frac{\mathcal{L}(y; \theta, \kappa) \Pi_0(\theta, u, \beta \mid \kappa) \Pi_0(\kappa)}{\int \mathcal{L}(y; \theta, \kappa) \Pi_0(\theta, u, \beta \mid \kappa) \Pi_0(\kappa) d(\theta, u, \beta, \kappa)}.$$

In this article, we focus on the case where the numerator is fully tractable, except for some normalizing constant invariant to $(\theta, u, \beta, \kappa)$. A clear advantage of this posterior, compared to that under the projected prior, is that we do not need to compute the projection $T(\beta)$ via iterative optimization, so the posterior computation is straightforward.

Since the quantity of interest is often only the marginal posterior of θ and κ , one can collect estimates of the joint posterior in the augmented space, then discard the information of u (Tanner and Wong, 1987). On the other hand, as we discussed above, having information about u can be useful for quantifying the difference between θ and the exact projection $T(\beta)$.

Finally, in the theory section, we will examine the large sample properties of the posterior under the gap-shrinkage prior carefully. For now, we conduct a simple analysis by examining the Hessian of the log-posterior, as is closely related to posterior uncertainty. Recall that the negative expected Hessian of the log-likelihood corresponds to the Fisher information matrix, whose inverse provides an asymptotic estimate of the covariance matrix for the parameters.

For simplicity, we focus on the proximal mapping case now,

$$\Pi(\theta, u, \kappa | y) \propto \underbrace{\mathcal{L}(y; \theta, \kappa) \pi_0^\beta(\theta + u) \Pi_0(\kappa)}_{=: \exp(-V(\theta, u, \kappa))} \exp[-\alpha\{g(\theta) + g^*(u) - u^\top \theta\}].$$

The observed negative Hessian given the data is

$$J(\theta, u, \kappa) = \nabla^2 V(\theta, u, \kappa) + \alpha \begin{bmatrix} \nabla^2 g(\theta) & -I & 0 \\ -I & \nabla^2 g^*(u) & 0 \\ 0 & 0 & 0 \end{bmatrix}. \quad (10)$$

By the Fenchel duality, at the primal-dual optimal $(\hat{\theta}, \hat{u})$, we have $\nabla^2 g^*(\hat{u}) = (\nabla^2 g(\hat{\theta}))^{-1}$. Therefore, at (θ, u) near $(\hat{\theta}, \hat{u})$, we have $\nabla^2 g(\theta) \nabla^2 g^*(u) - I \approx 0$. As a result, at a large α , the first 2×2 block of $J(\theta, u, \kappa)$ will be dominated by a close-to-singular matrix, corresponding to a nearly deterministic relation between θ and u . This is coherent with our intuition that a large α forces the (θ, u) to be close to the primal-dual optimizer space $\{(\theta, u) : g(\theta) + g^*(u) - u^\top \theta = 0\}$.

3 Posterior computation with Gibbs samplers

The posterior under a gap-shrinkage prior is a continuous density on Euclidean space and, in principle, can be estimated with gradient-based Hamiltonian Monte Carlo (Neal, 2011; Hoffman and Gelman, 2014). However, in practice we find that vanilla HMC is often a poor default: the dual variables enlarge the state by at least the number of dual coordinates, and for large α the log-posterior Hessian has an almost singular (θ, u) block as in Equation (10), reflecting motion along the near-deterministic zero-gap manifold. Without problem-specific preconditioning or splitting, trajectories are short and expensive.

We therefore use blocked Gibbs or Metropolis-within-Gibbs schemes that exploit conditional structure. The Gibbs samplers often have low per-iteration computational cost relative to HMC, which evaluates gradients and simulates trajectories at many intermediate points. The traditional tradeoff was implementation cost: deriving and coding problem-specific full conditionals is more time-consuming than invoking a generic HMC backend. However, coding assistants powered by large language models (LLMs) now greatly reduce the time needed to implement these schemes, so a blocked Gibbs sampler can be very competitive in total time.

We therefore state the general recipe below. The recipe can be used as a guideline for implementation or a natural-language prompt when generating sampler code via LLMs:

- (i) Likelihood augmentation for discrete responses. If the response is discrete, introduce latent variables so that, conditional on augmentation, the mean structure is linear in θ (Albert and Chib, 1993; Polson et al., 2013).
- (ii) Primal-side augmentation for nonsmooth g . When g is nonsmooth, such as based on separable ℓ_1 -norm functions, we can represent the penalty on $g(\theta)$ through a Gaussian scale mixture. For example, use the inverse-Gaussian or exponential mixtures employed in Bayesian lasso literature (Park and Casella, 2008), so that the θ -block is Gaussian conditional on the local scales.
- (iii) Blocked updates for θ . Update θ from its multivariate Gaussian full conditional, either jointly or one predictor at a time.
- (iv) Dual-variable updates. For the dual variables u , work with the exact one-dimensional conditional when available; in our examples, these conditionals are piecewise truncated-Gaussian and can be sampled coordinatewise.
- (v) Coordinate-wise slice sampling for remaining parameters.

This template is not unique, one could include gradient-based updates such as Metropolis-adjusted Langevin algorithm on some coordinates. Further, if one can integrate out some parameters analytically to allow further blocking, the sampler can be made more efficient. See discussion in (Bhattacharya et al., 2016).

4 Theory on posterior consistency and contraction rate

The gap-shrinkage prior in (4) is a relaxation of the exact projected prior. The exact projected prior is supported on the image of the projection map $T(\beta)$, while the gap-shrinkage prior assigns mass to (θ, u, β) with duality gap ≥ 0 , including values $\theta \neq T(\beta)$. This raises a natural concern: even though Theorems 1 and 2 show that a small gap implies that θ is close to the exact projection, as the sample size $n \rightarrow \infty$, does the posterior under the relaxed prior still concentrate at the true parameter θ_0 ?

To address this question, we focus on the setting $Y_1, \dots, Y_n \stackrel{\text{iid}}{\sim} p_{\theta_0}$, where the true parameter θ_0 lies in the projected set $\mathcal{M} = \{T(\beta) : \beta \in \mathbb{R}^p\}$, including the possibility that θ_0 is on the boundary of \mathcal{M} . In this section, Y_i is synonymous with y_i , but we use the capital letter to emphasize that it is a random variable on which we describe the convergence in probability $P_{\theta_0}^n$. Suppose that under the exact projected prior, the posterior is consistent at θ_0 . This is the baseline we consider: if the exact projected prior itself does not concentrate at θ_0 , then no comparison with its relaxation is meaningful.

4.1 Posterior consistency

We first show that the relaxed posterior is also consistent under a standard prior support condition. Let

$$G(\theta, u, \beta) := f(\theta; \beta) - d(u; \beta) \geq 0$$

denote the duality gap. Since $G(\theta, u, \beta) = 0$ if and only if $\theta = T(\beta)$ and u is dual optimal, the gap-shrinkage prior assigns positive mass to arbitrarily small neighborhoods of the

exact projected set whenever its base prior does. Therefore, if the exact projected prior is consistent because it places sufficient mass near θ_0 , then the relaxed prior inherits the same local support near θ_0 . We now formally state the theorem.

Theorem 3. *Assume that $Y_1, \dots, Y_n \stackrel{\text{iid}}{\sim} p_{\theta_0}$, where $\{p_\theta : \theta \in \Theta\}$ is dominated by a common σ -finite measure, and let ρ be a metric on Θ . Suppose that the model satisfies the conditions of Schwartz's consistency theorem (Schwartz, 1965; Barron et al., 1999) using the metric ρ . Further assume that for every $\eta > 0$, the gap-shrinkage prior assigns positive mass to*

$$\left\{ (\theta, u, \beta) : G(\theta, u, \beta) = 0, \text{KL}(p_{\theta_0}, p_\theta) < \eta \right\}.$$

where $\text{KL}(p_{\theta_0}, p_\theta) := \int \log \left(\frac{p_{\theta_0}}{p_\theta} \right) p_{\theta_0} d\mu$. Then the posterior under the gap-shrinkage prior is consistent at θ_0 , that is, for every $\epsilon > 0$, the posterior

$$\Pi_n(\rho(\theta, \theta_0) > \epsilon \mid Y_{1:n}) \stackrel{P_{\theta_0}^n}{\rightarrow} 0.$$

Theorem 3 shows that the relaxation does not compromise posterior consistency so long as the gap-shrinkage prior preserves sufficient Kullback–Leibler support near the truth through its zero-gap component. This is particularly relevant when the true parameter θ_0 lies on the boundary of \mathcal{M} : in such cases, nearby values outside \mathcal{M} may be arbitrarily close in Euclidean distance, so exact support is not the essential issue for consistency.

4.2 Contraction rate

We now turn to contraction rates. Suppose that under the exact projected prior, the posterior contracts at rate ε_n under the metric ρ , in the sense that for every sufficiently large $M > 0$, $\Pi^{\text{ex}}(\rho(T(\beta), \theta_0) > M\varepsilon_n \mid Y_{1:n}) \rightarrow 0$ in $P_{\theta_0}^n$ -probability. For the relaxed posterior, the concern is that the additional discrepancy between θ and $T(\beta)$ may deteriorate this rate. Intuitively, by the triangle inequality,

$$\rho(\theta, \theta_0) \leq \underbrace{\rho(\theta, T(\beta))}_{\text{relaxation error}} + \underbrace{\rho(T(\beta), \theta_0)}_{\text{projection error}}.$$

Therefore, the contraction rate could be established if both terms on the right-hand side are of ε_n scale. In the following, we proceed in two steps by first showing $G(\theta, u, \beta)$ is of ε_n^2 scale hence enabling the possibility of $\rho(\theta, T(\beta)) \downarrow 0$ at an ε_n rate by Theorem 1; we then establish the sufficient conditions for $\rho(T(\beta), \theta_0) \downarrow 0$ at the same rate.

First, the factor $\exp\{-\alpha_n G(\theta, u, \beta)\}$ promotes small gaps hence small $\rho(\theta, T(\beta))$ as *a priori*, but it does not guarantee rate ε_n for $\rho(\theta, T(\beta))$ in the posterior. Therefore, we need some technical conditions.

Theorem 4. *Consider the following conditions.*

- (i) *There exists a sequence $\varepsilon_n \rightarrow 0$ such that $n\varepsilon_n^2 \rightarrow \infty$.*
- (ii) *There exists a sieve $\mathcal{F}_n \subseteq \Theta \times \mathcal{U} \times \mathbb{R}^p$ such that $\Pi_n((\theta, u, \beta) \in \mathcal{F}_n \mid Y_{1:n}) \stackrel{P_{\theta_0}^n}{\rightarrow} 1$.*
- (iii) *There exist constants $C_1, C_2 > 0$ and measurable sets $B_n \subseteq \Theta \times \mathcal{U} \times \mathbb{R}^p$ such that $\Pi_0(B_n) \geq e^{-C_1 n \varepsilon_n^2}$, and for every $(\theta, u, \beta) \in B_n$,*

$$\text{KL}(p_{\theta_0}, p_\theta) \leq C_2 \varepsilon_n^2, \quad V(p_{\theta_0}, p_\theta) \leq C_2 \varepsilon_n^2, \quad G(\theta, u, \beta) \leq C_2 \varepsilon_n^2,$$

where $V(p_{\theta_0}, p_\theta) = \int \left[\log \left(\frac{p_{\theta_0}}{p_\theta} \right) \right]^2 p_{\theta_0} d\mu$ is the KL variance.

(iv) There exist a deterministic sequence $\kappa_n > 0$ and a constant $C_4 > 0$ such that, uniformly over $(\theta, u, \beta) \in \mathcal{F}_n$,

$$\ell_n(T(\beta)) - \ell_n(\theta) \geq \kappa_n G(\theta, u, \beta) - C_4 n \varepsilon_n^2,$$

where $\ell_n(\theta) = \sum_{i=1}^n \log p_\theta(Y_i)$.

(v) The constant α_n satisfies $\liminf_{n \rightarrow \infty} (\alpha_n + \kappa_n) \varepsilon_n^2 > 0$.

Under (i)-(v), for every sufficiently large $M > 0$,

$$\Pi_n(G(\theta, u, \beta) > M \varepsilon_n^2 \mid Y_{1:n}) \xrightarrow{P_{\theta_0}^n} 0.$$

Theorem 4 gives a useful guide for choosing the shrinkage parameter α_n . The quantity κ_n measures how strongly the likelihood itself favors the exact projection over a nonzero-gap value, while α_n is the additional regularization supplied by the prior. Thus the relevant quantity is not α_n alone, but rather the combined strength $\alpha_n + \kappa_n$. If the likelihood already contributes at the scale ε_n^{-2} , then fixed $\alpha_n \equiv \alpha$ is enough to preserve the exact projected-prior rate. In contrast, if the likelihood does not adequately penalize the duality gap, then α_n must increase with n to compensate. In this sense, adapting α_n is only necessary when the likelihood is too weak to dominate the residual relaxation error.

A useful rule of thumb follows immediately. In regular parametric models, one often has $\varepsilon_n = n^{-1/2}$. Therefore, rate preservation requires $\alpha_n + \kappa_n \gtrsim n$. If $\kappa_n \asymp n$, then any fixed $\alpha > 0$ is asymptotically sufficient. If $\kappa_n = O(1)$, then one needs $\alpha_n \asymp n$ to preserve the $n^{-1/2}$ contraction rate. The same reasoning extends to slower nonparametric rates by replacing $n^{-1/2}$ with the corresponding ε_n .

Next, we bound the distance between $T(\beta)$ and θ_0 under the relaxed posterior. There is a key distinction between $\Pi^{\text{ex},\beta}(\cdot \mid Y_{1:n})$ under the exact projected prior and $\Pi_n^{\text{rel},\beta}(\cdot \mid Y_{1:n})$ under the relaxed prior: under the exact projected prior, the likelihood is evaluated at $\theta = T(\beta)$, whereas under the relaxed prior it is evaluated at a relaxation θ of $T(\beta)$. As a result, contraction of $T(\beta)$ under the exact projected prior does not automatically transfer to the relaxed posterior; on the other hand, if the two posterior laws on β are asymptotically equivalent, then the contraction of $T(\beta)$ under the exact projected prior does transfer to the relaxed posterior.

Theorem 5. *Suppose there exists a measurable set $\mathcal{B}_n \subseteq \mathbb{R}^p$ and a deterministic sequence $\delta_n \rightarrow 0$ such that $\Pi_n^{\text{ex},\beta}(\mathcal{B}_n \mid Y_{1:n}) \xrightarrow{P_{\theta_0}^n} 1$ and*

$$P_{\theta_0}^n \left(\sup_{\beta \in \mathcal{B}_n} \left| \frac{m_n^{\text{rel}}(\beta)}{c_n \exp\{\ell_n(T(\beta))\}} - 1 \right| \leq \delta_n \right) \rightarrow 1. \quad (11)$$

for some deterministic $c_n > 0$ and $m_n^{\text{rel}}(\beta) := \iint \exp\{\ell_n(\theta)\} \exp\{-\alpha_n G(\theta, u, \beta)\} d\theta du$. Then

$$\|\Pi_n^{\text{rel},\beta}(\cdot \mid Y_{1:n}) - \Pi_n^{\text{ex},\beta}(\cdot \mid Y_{1:n})\|_{\text{TV}} \xrightarrow{P_{\theta_0}^n} 0.$$

Consequently, if for every sufficiently large $M > 0$, $\Pi_n^{\text{ex},\beta}(\rho(T(\beta), \theta_0) > M \varepsilon_n \mid Y_{1:n}) \xrightarrow{P_{\theta_0}^n} 0$, then also

$$\Pi_n^{\text{rel},\beta}(\rho(T(\beta), \theta_0) > M \varepsilon_n \mid Y_{1:n}) \xrightarrow{P_{\theta_0}^n} 0.$$

The condition (11) can hold under reasonable assumptions, such as appropriate local smoothness of the likelihood around the zero-gap point. In the interest of keeping the main exposition clear, we defer further theory development to the supplementary materials. With the above ingredients, we can now establish the contraction rate of the relaxed posterior.

Theorem 6. *Suppose the assumptions of Theorems 4 and 5 hold. Further assume that there exists a constant $C > 0$ such that $\rho(\theta, \theta_0) \leq C\|\theta - T(\beta)\|_2 + \rho(T(\beta), \theta_0)$. Then, for every sufficiently large $M > 0$,*

$$\Pi_n(\rho(\theta, \theta_0) > M\varepsilon_n \mid Y_{1:n}) \xrightarrow{P_{\theta_0}^n} 0.$$

In summary, the gap-shrinkage prior can match the large-sample behavior of the exact projected prior: consistency holds if the relaxed prior has enough KL support near the truth, while matching the contraction rate further requires (i) having the duality gap vanish rapidly and (ii) having the relaxed and exact posteriors for $T(\beta)$ be close. The tasks (i) and (ii) could be achieved by choosing appropriate shrinkage parameter α_n in a potentially diverging manner. An interesting alternative is the hybrid relaxation-projection approach, where a fixed value $\alpha_n = \alpha$ is used during posterior computation, and the projection $T(\beta)$ is applied in a post-processing step on the Markov chain samples after they have converged. Since this alternative is more of theoretical interest and is beyond the methodological scope of this article, we leave it for future work.

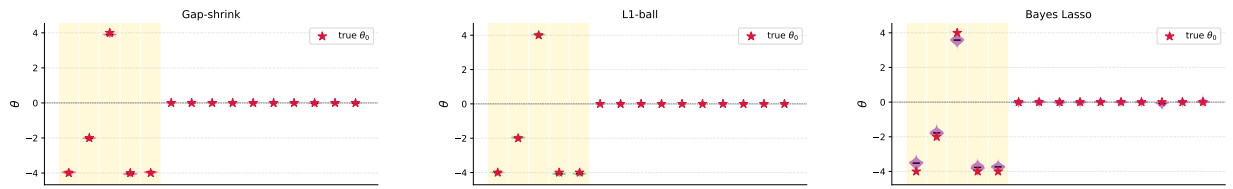
5 Simulation Studies

5.1 Sparse regression

We conduct experiments in a sparse linear regression setting with $n = 200$ observations and $p = 500$ predictors. The design matrix has $x_{ij} \sim N(0, 1)$, and the true coefficient vector $\theta_0 \in \mathbb{R}^p$ is sparse with 5 nonzero entries drawn uniformly from $\{-4, -2, 2, 4\}$; the response $y_i = x_i^\top \theta_0 + \varepsilon_i$ with $\varepsilon_i \sim N(0, 1)$. We use the Inverse-Gamma(2, 1) prior for λ .

We compare three methods that admit data-augmented Gibbs samplers, the gap-shrinkage prior ($\alpha = 1000$), the Bayesian lasso (Park and Casella, 2008), and the Generalized Double Pareto (GDP) prior (Armagan et al., 2013) in its hierarchical Laplace form; in addition, we also compare with the ℓ_1 -ball projected prior model. For these three methods the full conditionals are available in closed form, enabling exact Gibbs updates with no gradient evaluations. The ℓ_1 -ball projected prior (Xu and Duan, 2023) is fit with NUTS; its projection step (a sorting subroutine) must be executed at every leapfrog evaluation, making it more expensive per iteration. Each experiment is repeated over 20 independent replications with 1000 warmup and 1000 sampling iterations.

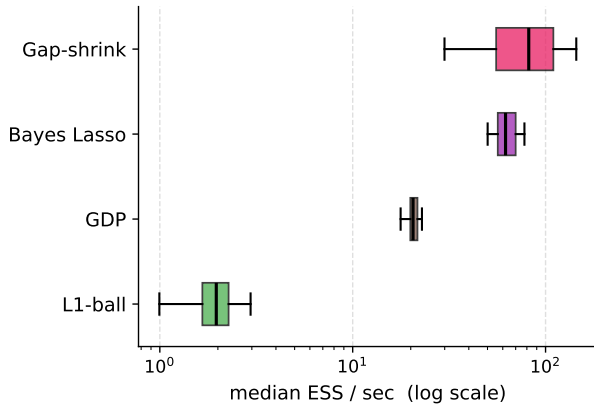
Figure 1(b-c) shows violin plots of posterior samples of θ for 15 selected coefficients under the gap-shrinkage prior and the ℓ_1 -ball prior. The gap-shrinkage prior concentrates its mass near the ground truth and correctly identifies the sparse support, closely matching the exact ℓ_1 -ball projected posterior. The GDP posterior is qualitatively similar and is not shown separately. The Bayesian lasso posterior shows inadequate shrinkage and biases for those nonzero coefficients. Figure 1(d) compares the effective sample size (ESS) per second across methods. The gap-shrinkage Gibbs sampler achieves the highest ESS per second (median ≈ 82), followed by the Bayesian lasso Gibbs (median ≈ 62) and GDP Gibbs (median ≈ 21). The ℓ_1 -ball NUTS sampler is far slower (median ≈ 2 ESS/sec) due to the overhead of repeated projection evaluations inside each leapfrog step. The autocorrelation function (ACF) boxplot in Figure 1(e) shows that the gap-shrinkage Gibbs sampler achieves rapid mixing. The autocorrelation drops below 0.2 within approximately 5 lags and is effectively zero by lag 15, indicating near-independence of successive draws and explaining high ESS.



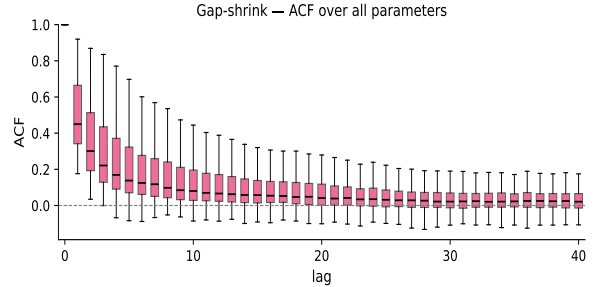
(a) Posterior samples of θ under gap-shrinkage prior.

(b) Posterior samples of θ under ℓ_1 -ball projected prior.

(c) Posterior samples of θ under Bayesian lasso.



(d) Median ESS per second.



(e) ACF boxplots (pooled over all p parameters) under gap-shrinkage prior show rapid decay in autocorrelation.

Figure 1: Sparse regression results ($n = 200$, $p = 500$, 20 replications).

5.2 Low-rank and sparse matrix smoothing

We next conduct experiments for a low-rank and sparse matrix smoothing problem, where we impose a simultaneous low-rank and sparse structure on the matrix $\theta \in \mathbb{R}^{p_1 \times p_2}$. This arises in robust PCA-type problems where one seeks a matrix that is simultaneously low-rank and elementwise sparse.

Specifically, one may obtain such a projection from $\beta \in \mathbb{R}^{p_1 \times p_2}$ to θ , using the proximal mapping with $g(\theta) = \lambda_1 \|\theta\|_* + \lambda_2 \|\theta\|_1$ for $\theta \in \mathbb{R}^{p_1 \times p_2}$, where $\|\cdot\|_1$ denotes the elementwise ℓ_1 norm, and $\|\cdot\|_*$ denotes the nuclear norm, the sum of the singular values typically computed via singular value decomposition (SVD). Such a projection problem is expensive to solve, since each SVD computation has a cubic complexity $O(p_1 p_2 \min(p_1, p_2))$ time, and the solution can only be computed via iterative algorithms such as ADMM, hence motivating the relaxation of projected priors.

Combining the results developed from Examples 4 and 5, we have the variational gap

$$\tilde{G}(\theta = AB^\top, V_1, V_2; \beta) = \frac{\lambda_1}{2} (\|A\|_F^2 + \|B\|_F^2) + \lambda_2 \|AB^\top\|_1 - \langle V_1 + V_2, AB^\top \rangle,$$

with both $V_1, V_2 \in \mathbb{R}^{p_1 \times p_2}$ and $\|V_1\|_{\text{op}} \leq \lambda_1$ and $|(V_2)_{ij}| \leq \lambda_2$ for all i, j ; $A \in \mathbb{R}^{p_1 \times r}$ and $B \in \mathbb{R}^{p_2 \times r}$ for some $r \geq 1$. Under sufficiently large λ_1 , we know the exact projection θ has a low rank, hence allowing us to use r smaller than p_1 and p_2 .

To simulate data, we use $p_1 = 50$, $p_2 = 40$, and first construct a ground-truth matrix $\theta_0 \in \mathbb{R}^{p_1 \times p_2}$ of rank 3 and elementwise sparsity 96.2%: three rank-one blocks of amplitudes 10, 7, and 4 are placed at non-overlapping 5×5 submatrices, and all other entries are zero ($\|\theta_0\|_F = 12.85$). The data are drawn i.i.d. via

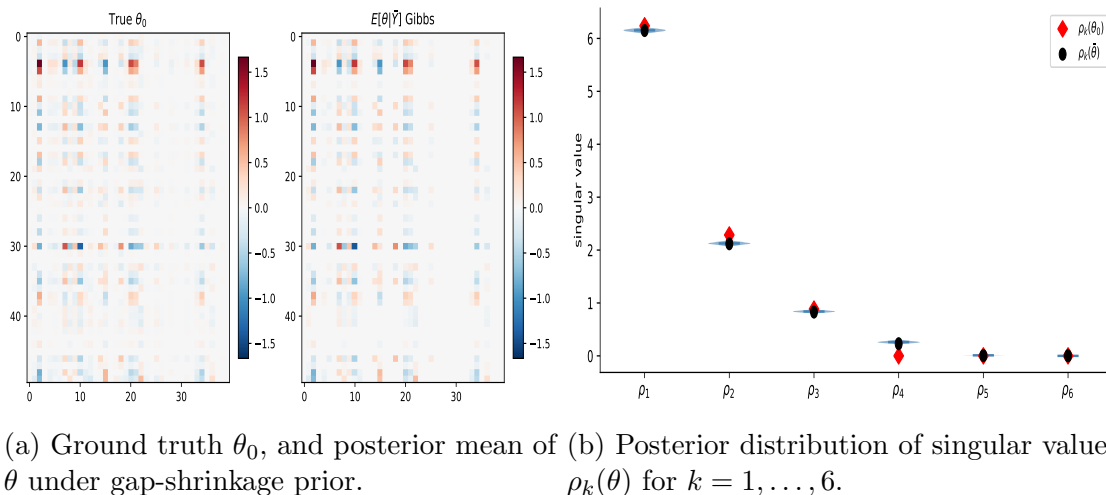
$$Y_s = \theta_0 + \varepsilon_s, \quad \varepsilon_s \sim \mathcal{N}(0, \sigma^2 I_{p_1} \otimes I_{p_2}),$$

for $s = 1, \dots, S$ with $S = 100$, $\sigma = 0.3$.

We use matrix Gaussian likelihood consistent with the data simulation, and assign inverse-gamma prior for σ^2 , and relaxed projection prior for the matrix θ with dimension $r = 5$, and elements $\beta_{ij} \sim N(0, 100)$. In the posterior computation, we develop a Gibbs sampler (with details provided in the supplementary materials). For the operator norm constraint on V_1 , we enforce it by simply reparameterizing $\lambda_1 = \|V_1\|_F \geq \|V_1\|_{\text{op}}$.

We run 3000 warmup and 3000 sampling iterations. Figure 2 shows the posterior mean of the estimated θ , and the posterior distribution of the singular values $\rho_k(\theta)$ of θ . The posterior singular values $\rho_k(\theta)$ concentrate tightly around the true values for $k = 1, 2, 3$, while the posterior for $k \geq 4$ collapses to near zero, reflecting automatic rank selection. The noise variance σ^2 is recovered accurately, with posterior mean 0.092. The results show that the gap-shrinkage prior handles simultaneous constraints and correctly identifies matrix rank and sparsity.

In terms of the computational costs, the Gibbs sampler for the gap-shrinkage prior took 29 seconds. For comparison, we also ran the model with the exact projected prior, using ADMM to solve the projection step. This approach required 4 hours to complete 6,000 iterations, which is substantially slower than the gap-shrinkage Gibbs sampler.



(a) Ground truth θ_0 , and posterior mean of θ under gap-shrinkage prior. (b) Posterior distribution of singular values $\rho_k(\theta)$ for $k = 1, \dots, 6$.

Figure 2: Results for low-rank and sparse matrix smoothing.

6 Data Application

We now apply the gap-shrinkage model to household-level grocery purchase data from the 2020 Nielsen Consumer Panel. We use the shopping records from $H = 793$ households who made $n = 803$ trips to grocery retailers, purchasing items from $m = 26$ product subcategories under six departments: alcoholic beverages, dairy, deli, fresh produce, frozen foods, and packaged meat. Each response is a binary vector $y_i \in \{0, 1\}^m$ indicating whether each of the $m = 26$ subcategories was purchased on trip i . The data include several covariates: standardized total spending, total quantity, average paid price, quarters (Q1, Q2, Q3, Q4), and regions (Midwest, Northeast, South, West) derived from store ZIP code; in total, they correspond to $p = 9$. For these multivariate binary responses, we use the probit model

$$y_{ij} \sim \text{Bernoulli}[\Phi(\mu_{ij})], \quad \mu_i = \theta x_i + W \gamma_{h(i)},$$

where i is shopping trip, j is product subcategory, $h(i)$ is household for trip i , and $\mu_i \in \mathbb{R}^m$. $\theta \in \mathbb{R}^{m \times p}$ is the category-by-covariate coefficient matrix, Φ is the standard Gaussian distribution function, $W \gamma_{h(i)}$ captures the household-specific random effect, $W \in \mathbb{R}^{m \times d}$ is a category loading matrix, and $\gamma_h \in [0, \infty)^d$ is a household-specific latent effect.

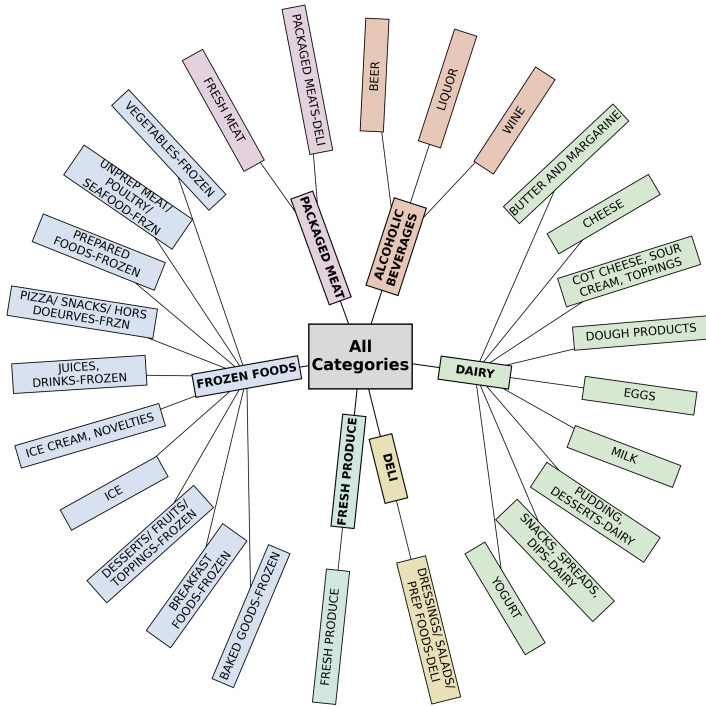


Figure 3: Taxonomy of the 26 subcategories used in the data application. The radial layout highlights the departmental block structure used to define stronger within-department smoothing and a learned cross-department smoothing weight.

Since the coefficient matrix θ has 234 elements, we impose a taxonomy-based smoothing prior across categories. The taxonomy is shown in Figure 3. Let $G = (V, E)$ be a complete weighted graph on the m subcategories, where $V = \{1, \dots, m\}$. We fix the weight $\lambda_{j,j'} = 1$ when the two subcategories belong to the same department and use a smaller weight $\lambda_{j,j'} = \omega_{\text{cross}} \in (0, 1)$ otherwise. Let $B \in \mathbb{R}^{|E| \times m}$ be a directed incidence matrix and let Λ denote the corresponding diagonal matrix of edge weights. Then smoothing using the weighted graph corresponds to the proximal loss

$$f(z; \beta) = \frac{1}{2} \|\beta - z\|_F^2 + \rho \|\Lambda B z\|_{1,1},$$

where $\|\cdot\|_{1,1}$ denotes the entrywise ℓ_1 norm. For edge $e = (j, j')$, $B_{e,k} = +1$ if $k = j$, $B_{e,k} = -1$ if $k = j'$, and $B_{e,k} = 0$ otherwise. Each row of Bz computes the difference $z_j - z_{j'}$ along one edge. The corresponding gap-shrinkage prior takes the form

$$\Pi_0(\theta, v, \beta \mid \rho) \propto \exp \left[-\alpha \left\{ \rho \|\Lambda B \theta\|_{1,1} - \langle \theta, B^\top \Lambda v \rangle \right\} \right] \pi_0^\beta(\beta),$$

subject to $\theta = \beta - B^\top \Lambda v$ and $|v_{e,k}| \leq \rho$. We set the prior for global smoothing strength $\rho \sim \text{Inverse-Gamma}(2, 1)$, cross-department weight $\omega_{\text{cross}} \sim \text{Beta}(1, 1)$, $d = 5$ for the low-dimensional random effect structure, a Gaussian prior on W , and independent half-Gaussian priors on the coordinates of γ_h . Since θ is on the probit scale, heavy tails are not expected a priori, so we use a Gaussian prior kernel $\pi_0^\beta(\beta) \propto \exp\{-\|\beta\|_F^2/200\}$ for computational convenience.

Since the smoothing is applied on the complete graph, note the following identity for the term within each department J_g

$$\sum_{j < j': j, j' \in J_g} \rho |\theta_{j,k} - \theta_{j',k}| = \rho \sum_{t=1}^{m_g} |2t - m_g - 1| |\theta_{(t),k} - c_g|,$$

where c_g is the sample median, and $\theta_{(t),k}$ is the t -th order statistic of $\{\theta_{j,k}\}_{j \in J_g}$. Therefore, there is an increasing shrinkage effect for the coefficient away from the median.

We ran 1000 warmup iterations followed by 10000 retained draws. The fitted gap-shrinkage model yields a posterior mean of smoothing strength as $\rho \approx 0.0045$, while the cross-department weight is driven close to zero, with a posterior mean of $\omega_{\text{cross}} \approx 2.8 \times 10^{-4}$. Thus, the posterior favors smoothing within departments while applying almost no smoothing across departments. For the nine predictors, the posterior means of the subcategory coefficients are shown as boxplots in Figure 4.

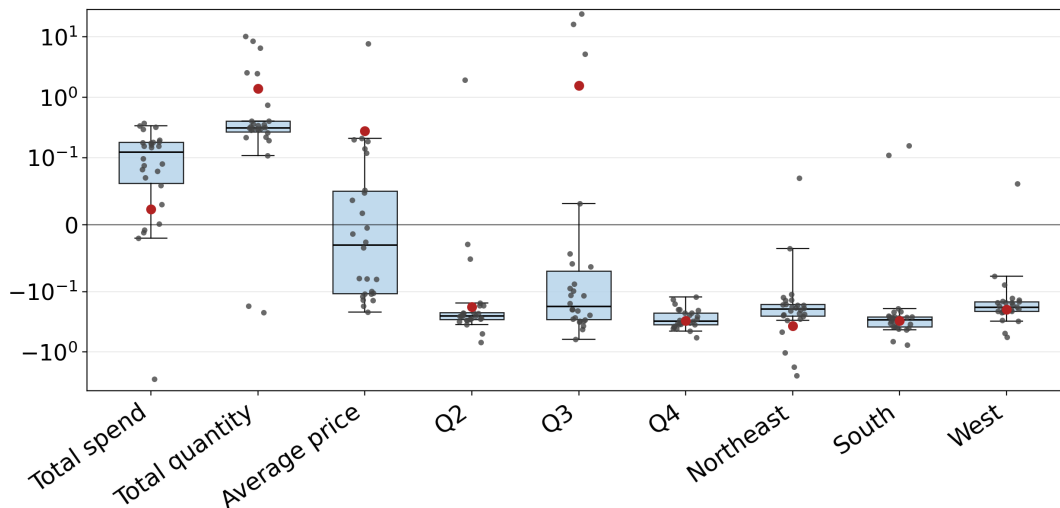


Figure 4: Distribution across the 26 subcategories of the posterior mean coefficient for each predictor under the gap-shrinkage model. The red dots mark the across-category posterior mean for each predictor.

Figure 5 shows four selected heatmaps of the absolute pairwise differences that are especially interpretable in this application. Each cell in a heatmap shows how differently two subcategories respond to a covariate. For total quantity, PUDDING, DESSERTS-DAIRY stands out because its posterior mean coefficient is strongly positive relative to nearly all other subcategories. For average price, LIQUOR is the dominant outlier, which is consistent with the fact that liquor purchases tend to be associated with higher average prices. For the third-quarter indicator (July–September), ICE shows an exceptionally large positive coefficient, which distinguishes it from the other seasonal indicators reported in the Supplementary Materials, suggesting distinctly higher purchase probability in Q3. By contrast, the West region indicator is much more homogeneous overall; however, WINE remains noticeably more negative than FRESH PRODUCE and most other subcategories.

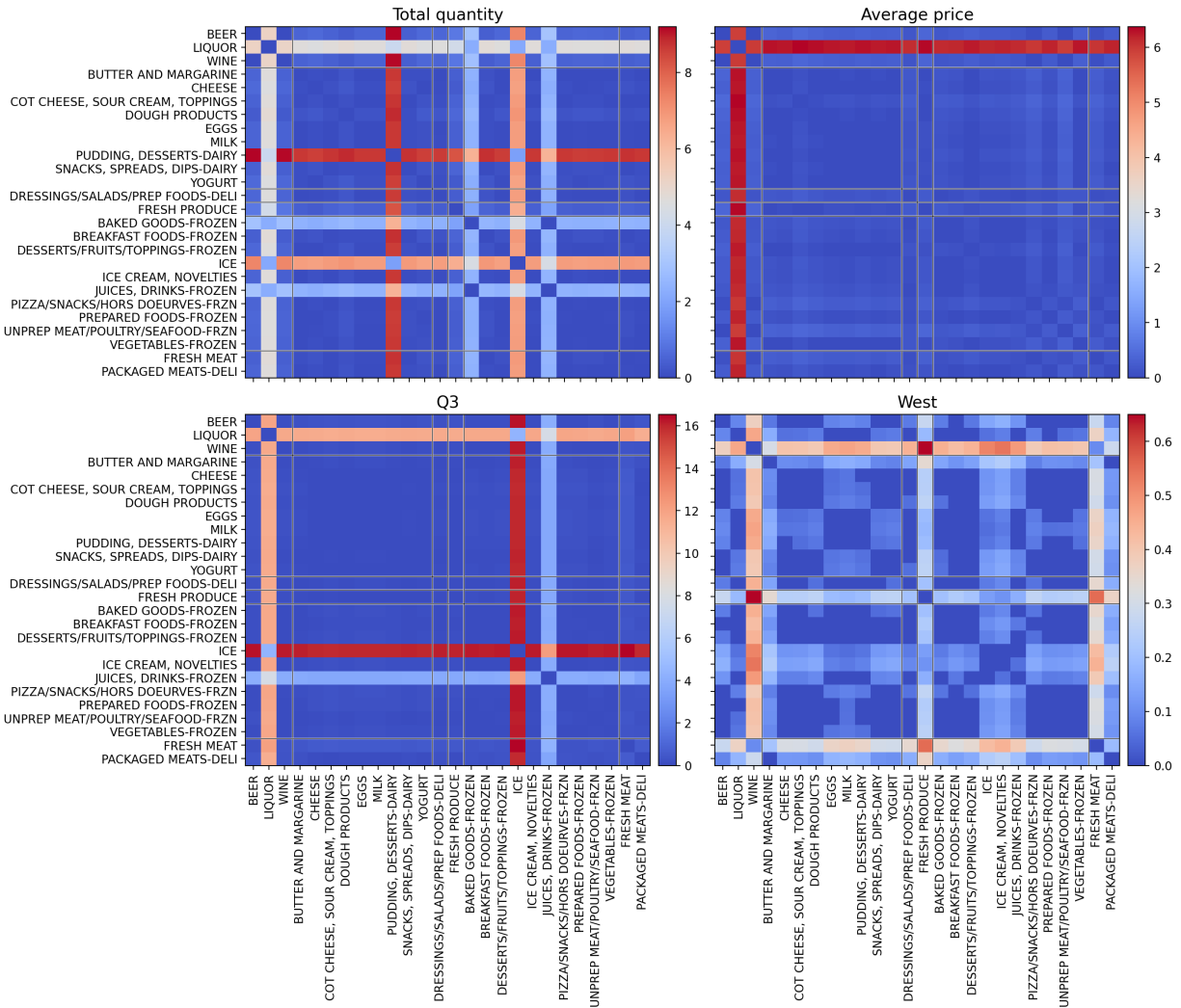
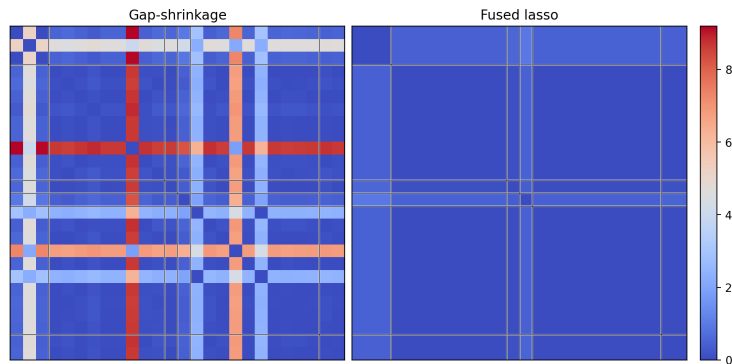


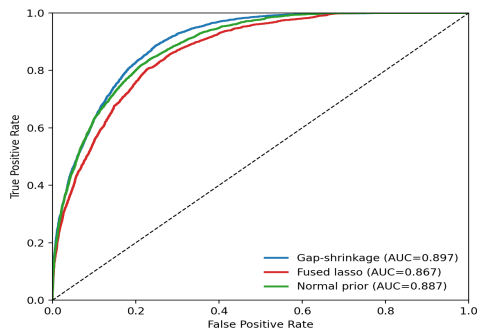
Figure 5: Four selected heatmaps of absolute pairwise posterior mean differences under the gap-shrinkage model, ordered by department.

For comparison, we fit two alternate models, with the same likelihood and latent household term, but different priors on θ : (i) a Bayesian fused-lasso prior with $\pi_0^\theta(\theta \mid \rho) \propto \exp\{-\rho\|\Lambda B\theta\|_{1,1}\}$, and retaining the same prior for ρ and ω_{cross} ; (ii) an independent Gaussian prior with $\pi_0^\theta(\theta) \propto \exp\{-\|\theta\|_F^2/200\}$. Under the Bayesian fused-lasso prior, the model drives ρ to an extremely large scale, with posterior mean about 9.94×10^6 , while pushing the cross-department weight to a posterior mean of about 10^{-8} . As a result, the coefficient estimate under the Bayesian fused-lasso prior is much more homogeneous than the gap-shrinkage prior within department (Figure 6a). The predictive ranking performance of the Bayesian fused-lasso model is also weaker. Using posterior mean probit scores and pooling all trip-category outcomes, Figure 6(b) shows that the area under the ROC curve (AUC) is 0.867 for the Bayesian fused-lasso model, compared with 0.897 for the gap-shrinkage model. The independent Gaussian prior on θ gives AUC 0.887 but produces much more dispersed category-level coefficients.

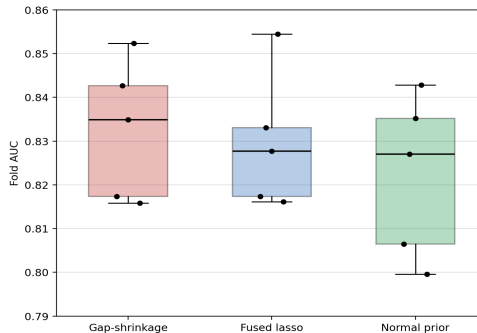
We also performed a 5-fold cross-validation using the same three models. The pooled AUCs are 0.832 for gap-shrinkage, 0.829 for the Bayesian fused-lasso prior, and 0.821 for the independent Gaussian prior. The foldwise distributions in Figure 6(c) show that out-of-sample differences are modest, but the gap-shrinkage prior remains slightly better overall while avoiding the over-smoothing behavior of the Bayesian fused-lasso fit and high dispersion in coefficients produced by the independent Gaussian prior with little pooling.



(a) Absolute pairwise posterior mean differences for the total quantity coefficient.



(b) ROC curves based on posterior mean probit scores.



(c) Boxplots of foldwise AUC values from the five-fold cross-validated comparison.

Figure 6: Comparison of the gap-shrinkage model with the Bayesian fused-lasso model and the independent Gaussian prior model on θ . (a) Absolute pairwise posterior mean differences for the total quantity coefficient; (b) ROC curves based on posterior mean probit scores; (c) Boxplots of foldwise AUC values from five-fold cross-validated comparison.

7 Discussion

In this article, we developed a gap-shrinkage prior that relaxes exact projected priors and bypasses an iterative projection subroutine inside MCMC. The gap-shrinkage prior keeps θ near the exact projection of β , while the randomness in β allows the projection target itself to vary continuously across the ambient space. This gives a useful compromise between exact projection enforcement and computational tractability. In particular, the prior preserves the interpretation of projected priors as concentrating mass near a useful target, but replaces a difficult constrained sampling problem by a continuous posterior on an enlarged space, a perspective that is reminiscent of the literature on Bayesian relaxation and probabilistic numerical methods (Cockayne et al., 2019; Duan et al., 2020; Matuk et al., 2022; Presman and Xu, 2023).

There are several interesting future directions worth further exploration. First, the close-to-deterministic relation between θ and β near the zero-gap manifold makes the model less suitable for generic gradient-based methods such as canonical Hamiltonian Monte Carlo. In these settings, the joint posterior geometry can become nearly singular in the (θ, u, β) coordinates, and this can lead to inefficient trajectories unless substantial problem-specific tuning is introduced. It would therefore be worthwhile to study extensions based on geometry-aware methods, such as preconditioned or Riemannian HMC (Girolami

and Calderhead, 2011), or hybrid samplers that combine gradient moves on some blocks with marginal or slice updates on others. Second, in this article, we considered projection onto a convex set. It would be interesting to consider projection onto nonconvex sets as well, for example, those arising in principal-curve (Hastie and Stuetzle, 1989) or manifold-type models, although in such settings identifiability, multimodality, and local geometry would require substantially more careful treatment. Third, the current connection between gap-shrinkage and the global-local prior literature suggests a broader view of Bayesian shrinkage: instead of shrinking coefficients toward zero, one can shrink them toward a lower-dimensional structured set or manifold. In our setting, that structured target is the image of a projection map, but the same principle could be used more broadly to encode shrinkage toward low-dimensional manifolds, such as null spaces arising in hypothesis testing. Fourth, the push-forward construction in (2) shares a deep structural analogy with generative adversarial networks (Goodfellow et al., 2014) and semi-implicit variational inference (Yin and Zhou, 2018): all three frameworks define a distribution over a target variable by applying a deterministic or learned transformation to a simple latent variable, bypassing an explicit density on the output space. Exploring this connection may lead to new hybrid formulations that combine the statistical guarantees of gap-shrinkage priors with the flexibility of implicit generative models.

Disclosure of the use of generative AI: In preparing this paper, the authors used Claude Code to assist with code development and figure plotting. The authors take full responsibility for all content presented.

Acknowledgement: The research of Leo Duan is partially supported by the U.S. National Science Foundation under grant NSF-DMS 2319551.

References

- Agrell, C. (2019). Gaussian Processes with Linear Operator Inequality Constraints. *Journal of Machine Learning Research* 20(135), 1–36.
- Albert, J. H. and S. Chib (1993). Bayesian Analysis of Binary and Polychotomous Response Data. *Journal of the American Statistical Association* 88(422), 669–679.
- Armagan, A., D. B. Dunson, and J. Lee (2013). Generalized Double Pareto Shrinkage. *Statistica Sinica* 23(1), 119.
- Astfalck, L., D. Sen, S. Patra, E. Cripps, and D. B. Dunson (2024). Posterior Projection for Inference in Constrained Spaces. *arXiv preprint arXiv:1812.05741*.
- Barron, A., M. J. Schervish, and L. Wasserman (1999). The Consistency of Posterior Distributions in Nonparametric Problems. *The Annals of Statistics* 27(2), 536–561.
- Bauschke, H. H. and J. M. Borwein (1996). On projection algorithms for solving convex feasibility problems. *SIAM review* 38(3), 367–426.
- Bhattacharya, A., A. Chakraborty, and B. K. Mallick (2016). Fast Sampling with Gaussian Scale Mixture Priors in High-Dimensional Regression. *Biometrika*, asw042.
- Bhaumik, P., W. Shi, and S. Ghosal (2022). Two-step Bayesian Methods for Generalized Regression Driven by Partial Differential Equations. *Bernoulli* 28(3), 1625–1647.

- Boyle, J. P. and R. L. Dykstra (1986). A Method for Finding Projections onto the Intersection of Convex Sets in Hilbert Spaces. In *Advances in Order Restricted Statistical Inference: Proceedings of the Symposium on Order Restricted Statistical Inference held in Iowa City, Iowa, September 11–13, 1985*, pp. 28–47. Springer.
- Carvalho, C. M., N. G. Polson, and J. G. Scott (2009). Handling Sparsity via the Horseshoe. In *Proceedings of the Twelfth International Conference on Artificial Intelligence and Statistics*, Volume 5 of *Proceedings of Machine Learning Research*, pp. 73–80. PMLR.
- Cockayne, J., C. J. Oates, T. J. Sullivan, and M. Girolami (2019). Bayesian Probabilistic Numerical Methods. *SIAM Review* 61(4), 756–789.
- Duan, L. L., A. L. Young, A. Nishimura, and D. B. Dunson (2020). Bayesian Constraint Relaxation. *Biometrika* 107(1), 191–204.
- Duchi, J., S. Shalev-Shwartz, Y. Singer, and T. Chandra (2008). Efficient Projections onto the L1-Ball for Learning in High Dimensions. In *Proceedings of the 25th international conference on Machine learning*, pp. 272–279.
- Dunson, D. B. and B. Neelon (2003). Bayesian Inference on Order-Constrained Parameters in Generalized Linear Models. *Biometrics* 59(2), 286–295.
- Everink, J. M., Y. Dong, and M. S. Andersen (2023). Sparse Bayesian Inference with Regularized Gaussian Distributions. *Inverse Problems* 39(11), 115004.
- Fazel, M., H. Hindi, and S. P. Boyd (2001). A Rank Minimization Heuristic with Application to Minimum Order System Approximation. *Proceedings of the American Control Conference* 6, 4734–4739.
- Gelfand, A. E., A. F. M. Smith, and T.-M. Lee (1992). Bayesian Analysis of Constrained Parameter and Truncated Data Problems Using Gibbs Sampling. *Journal of the American Statistical Association* 87(418), 523–532.
- Ghosal, S., J. K. Ghosh, and A. W. van der Vaart (2000). Convergence Rates of Posterior Distributions. *The Annals of Statistics* 28(2), 500–531.
- Girolami, M. and B. Calderhead (2011). Riemann Manifold Langevin and Hamiltonian Monte Carlo Methods. *Journal of the Royal Statistical Society: Series B (Statistical Methodology)* 73(2), 123–214.
- Goodfellow, I. J., J. Pouget-Abadie, M. Mirza, B. Xu, D. Warde-Farley, S. Ozair, A. Courville, and Y. Bengio (2014). Generative Adversarial Nets. In *Advances in Neural Information Processing Systems*, Volume 27.
- Hadj-Amar, B., J. Jewson, and M. Vannucci (2024). Bayesian Sparse Vector Autoregressive Switching Models with Application to Human Gesture Phase Segmentation. *The Annals of Applied Statistics* 18(3), 2511–2531.
- Hastie, T. and W. Stuetzle (1989). Principal Curves. *Journal of the American Statistical Association* 84(406), 502–516.
- Hoffman, M. D. and A. Gelman (2014). The No-U-Turn Sampler: Adaptively Setting Path Lengths in Hamiltonian Monte Carlo. *Journal of Machine Learning Research* 15(1), 1593–1623.

- Kang, J., B. J. Reich, and A.-M. Staicu (2018). Scalar-on-Image Regression via the Soft-Thresholded Gaussian Process. *Biometrika* 105(1), 165–184.
- Li, Y., B. A. Craig, and A. Bhadra (2019). The Graphical Horseshoe Estimator for Inverse Covariance Matrices. *Journal of Computational and Graphical Statistics* 28(3), 747–757.
- Lin, L. and D. B. Dunson (2014). Bayesian Monotone Regression Using Gaussian Process Projection. *Biometrika* 101(2), 303–317.
- Matuk, J., A. H. Herring, and D. B. Dunson (2022). Bayesian Modeling of Nearly Mutually Orthogonal Processes. *arXiv preprint arXiv:2205.12361*.
- Mohammadi, A. and E. C. Wit (2015). Bayesian Structure Learning in Sparse Gaussian Graphical Models. *Bayesian Analysis* 10(1), 109 – 138.
- Neal, R. M. (2011). MCMC Using Hamiltonian Dynamics. In S. Brooks, A. Gelman, G. Jones, and X.-L. Meng (Eds.), *Handbook of Markov Chain Monte Carlo*, Chapter 5. CRC Press.
- Neelon, B. and D. B. Dunson (2004). Bayesian Isotonic Regression and Trend Analysis. *Biometrics* 60(2), 398–406.
- Pal, S. and S. Ghosal (2025). Projection-Posterior for Variable Selection: Weak Limit and Coverage. *Electronic Journal of Statistics* 19(2), 3743–3770.
- Park, T. and G. Casella (2008). The Bayesian Lasso. *Journal of the American Statistical Association* 103(482), 681–686.
- Peyré, G. and M. Cuturi (2019). *Computational Optimal Transport: With Applications to Data Science*. Now Foundations and Trends.
- Polson, N. G. and J. G. Scott (2011). Shrink Globally, Act Locally: Sparse Bayesian Regularization and Prediction. In J. M. Bernardo, M. J. Bayarri, J. O. Berger, A. P. Dawid, D. Heckerman, A. F. M. Smith, and M. West (Eds.), *Bayesian Statistics 9*, pp. 501–538. Oxford: Oxford University Press.
- Polson, N. G., J. G. Scott, and B. T. Willard (2015). Proximal Algorithms in Statistics and Machine Learning. *Statistical Science* 30(4), 559–581.
- Polson, N. G., J. G. Scott, and J. Windle (2013). Bayesian Inference for Logistic Models Using Pólya–Gamma Latent Variables. *Journal of the American Statistical Association* 108(504), 1339–1349.
- Presman, R. and J. Xu (2023). Distance-to-Set Priors and Constrained Bayesian Inference. In *Proceedings of The 26th International Conference on Artificial Intelligence and Statistics*, Volume 206 of *Proceedings of Machine Learning Research*, pp. 2310–2326. PMLR.
- Schwartz, L. (1965). On Bayes Procedures. *Zeitschrift für Wahrscheinlichkeitstheorie und Verwandte Gebiete* 4(1), 10–26.
- Scieur, D., G. Gidel, Q. Bertrand, and F. Pedregosa (2022). The Curse of Unrolling: Rate of Differentiating Through Optimization. *Advances in Neural Information Processing Systems* 35, 17133–17145.
- Tanner, M. A. and W. H. Wong (1987). The Calculation of Posterior Distributions by Data Augmentation. *Journal of the American Statistical Association* 82(398), 528–540.

- Thomas, A. M., M. Jauch, and D. S. Matteson (2025). Bayesian Changepoint Detection via Logistic Regression and the Topological Analysis of Image Series. *Technometrics*.
- Thompson, R., E. V. Bonilla, and R. Kohn (2024). ProDAG: Projection-Induced Variational Inference for Directed Acyclic Graphs. *arXiv preprint arXiv:2405.15167*.
- Xu, M. and L. L. Duan (2023). Bayesian Inference with the l1-Ball Prior: Solving Combinatorial Problems with Exact Zeros. *Journal of the Royal Statistical Society Series B: Statistical Methodology* 85(5), 1538–1560.
- Xu, M., H. Zhou, Y. Hu, and L. L. Duan (2024). Bayesian Inference Using the Proximal Mapping: Uncertainty Quantification Under Varying Dimensionality. *Journal of the American Statistical Association* 119(547), 1847–1858.
- Yin, M. and M. Zhou (2018). Semi-Implicit Variational Inference. In *International conference on machine learning*, pp. 5660–5669. PMLR.
- Zeng, Z., M. Li, and M. Vannucci (2024). Bayesian Image-on-Scalar Regression with a Spatial Global-Local Spike-and-Slab Prior. *Bayesian Analysis*.
- Zhou, X., Q. Heng, E. C. Chi, and H. Zhou (2024). Proximal MCMC for Bayesian Inference of Constrained and Regularized Estimation. *The American Statistician* 78(4), 379–390.

Supplementary Materials

A Proofs

A.1 Tail bound for gap-shrinkage prior for ℓ_1 -norm proximal loss

Lemma 1. *For the marginal prior $\pi_0(\theta|\lambda) = \prod_{j=1}^p \pi_0(\theta_j|\lambda)$, for $|\theta_j|$ sufficiently large, there exists a constant $C > 0$ such that, $\pi_0(\theta_j|\lambda) \geq C|\theta_j|^{-3}$.*

Proof. We first note that $1 + (\theta_j + u_j)^2 \leq 1 + (|\theta_j| + \lambda)^2$. Therefore,

$$\begin{aligned}
& \int \exp\{-\alpha(\lambda - |u_j|)|\theta_j|\} 1(|u_j| \leq \lambda) \{1 + (\theta_j + u_j)^2\}^{-1} du_j \\
& \geq \frac{1}{1 + (|\theta_j| + \lambda)^2} \int_{-\lambda}^{\lambda} \exp\{-\alpha(\lambda - |u_j|)|\theta_j|\} du_j \\
& = \frac{2}{1 + (|\theta_j| + \lambda)^2} \int_0^{\lambda} \exp\{-\alpha(\lambda - u_j)|\theta_j|\} du_j \\
& = \frac{2}{1 + (|\theta_j| + \lambda)^2} \int_0^{\lambda} e^{-\alpha t|\theta_j|} dt \\
& = \frac{2(1 - e^{-\alpha\lambda|\theta_j|})}{\alpha|\theta_j|\{1 + (|\theta_j| + \lambda)^2\}}.
\end{aligned}$$

Clearly, the right hand side is $\Omega(|\theta_j|^{-3})$ as $|\theta_j| \rightarrow \infty$. □

A.2 Proof of Theorem 2

Proof. Letting $\eta = \nabla\psi(\beta)$, the primal is

$$\min_{z \in \mathbb{R}^p} \psi(z) - \psi(\beta) - (z - \beta)^\top \eta + I_C(z) = \min_z \left\{ \psi(z) - z^\top \eta + I_C(z) \right\} + \beta^\top \eta - \psi(\beta).$$

Letting $h(z) = \psi(z) - z^\top \eta$, we have $h^*(v) = \sup_z \{v^\top z - \psi(z) + z^\top \eta\} = \psi^*(v + \eta)$, hence

$$h(z) = \sup_v v^\top z - h^*(v) = \sup_v v^\top z - \psi^*(v + \eta).$$

Ignoring constant $\beta^\top \eta - \psi(\beta)$, the effective primal is

$$\inf_z \sup_v v^\top z - \psi^*(v + \eta) + I_C(z).$$

Exchanging inf and sup, we have the effective dual problem:

$$\begin{aligned} \sup_v \inf_z v^\top z - \psi^*(v + \eta) + I_C(z) &= \sup_v \left\{ -\sup_z (-v^\top z - I_C(z)) \right\} - \psi^*(v + \eta) \\ &= \sup_v \{-\sigma_C(-v)\} - \psi^*(v + \eta). \end{aligned}$$

Replacing v by $-u$ and adding the constant term, we obtain the dual function as stated in the theorem.

Next, using the generalized Pythagorean inequality in Bregman projection, we have

$$D_\psi(z, \beta) \geq D_\psi(z, \hat{z}) + D_\psi(\hat{z}, \beta), \quad z \in C.$$

Rearranging terms and applying the weak duality, we have the stated inequality. \square

A.3 Proof of Theorem 3

Proof. The proof is straightforward, and we present it for completeness. Let $\tilde{\Pi}$ denote the prior on (θ, u, β) induced by the gap-shrinkage construction, and let Π denote its marginal prior on θ . By assumption, for every $\eta > 0$,

$$\tilde{\Pi}(\{(\theta, u, \beta) : G(\theta, u, \beta) = 0, KL(p_{\theta_0}, p_\theta) < \eta\}) > 0.$$

Marginalizing over u and β , we obtain $\Pi(\{\theta : KL(p_{\theta_0}, p_\theta) < \eta\}) > 0$ for every $\eta > 0$. Hence the marginal prior Π assigns positive mass to every KL neighborhood of θ_0 . Since the model is assumed to satisfy the conditions of Schwartz's consistency theorem, the KL-support property above implies posterior consistency under the prior Π . Therefore, for every $\epsilon > 0$, $\Pi_n(\rho(\theta, \theta_0) > \epsilon \mid Y_{1:n}) \xrightarrow{P_{\theta_0}^n} 0$. \square

A.4 Proof of Theorem 4

Proof. Write the relaxed posterior as

$$\Pi_n(A \mid Y_{1:n}) = \frac{N_n(A)}{D_n},$$

where

$$N_n(A) = \iiint_A \exp\{\ell_n(\theta)\} e^{-\alpha_n G(\theta, u, \beta)} \Pi_0(d\theta, du, d\beta), \quad D_n = N_n(\Theta \times \mathcal{U} \times \mathbb{R}^p).$$

1. Lower bound the denominator. Observe that

$$D_n = e^{\ell_n(\theta_0)} \iiint e^{\ell_n(\theta) - \ell_n(\theta_0)} e^{-\alpha_n G(\theta, u, \beta)} \Pi_0(d\theta, du, d\beta).$$

By assumption (iii), for $(\theta, u, \beta) \in B_n$ we have $G(\theta, u, \beta) \leq C_2 \varepsilon_n^2$, and therefore $D_n \geq e^{\ell_n(\theta_0)} e^{-\alpha_n C_2 \varepsilon_n^2} \iiint_{B_n} e^{\ell_n(\theta) - \ell_n(\theta_0)} \Pi_0(d\theta, du, d\beta)$.

By the standard marginal likelihood lower bound over Kullback–Leibler neighborhoods; see, e.g., Ghosal et al. (2000), assumption (iii) implies that there exists a constant $C > 0$ such that

$$P_{\theta_0}^n \left(\iiint_{B_n} e^{\ell_n(\theta) - \ell_n(\theta_0)} \Pi_0(d\theta, du, d\beta) \geq e^{-Cn\varepsilon_n^2} \right) \rightarrow 1.$$

Hence,

$$P_{\theta_0}^n (D_n \geq e^{\ell_n(\theta_0)} \exp\{-Cn\varepsilon_n^2 - \alpha_n C_2 \varepsilon_n^2\}) \rightarrow 1.$$

2. Upper bound the numerator. Consider the numerator over the large-gap set

$$A_{n,M} := \{(\theta, u, \beta) \in \mathcal{F}_n : G(\theta, u, \beta) > M\varepsilon_n^2\}.$$

For $(\theta, u, \beta) \in A_{n,M}$, assumption (iv) gives $\ell_n(\theta) \leq \ell_n(T(\beta)) - \kappa_n G(\theta, u, \beta) + C_4 n \varepsilon_n^2$, hence

$$e^{\ell_n(\theta)} e^{-\alpha_n G(\theta, u, \beta)} \leq e^{\ell_n(T(\beta))} e^{-(\alpha_n + \kappa_n)G(\theta, u, \beta) + C_4 n \varepsilon_n^2} \leq e^{C_4 n \varepsilon_n^2 - (\alpha_n + \kappa_n)M\varepsilon_n^2} e^{\ell_n(T(\beta))}.$$

Therefore,

$$N_n(A_{n,M}) \leq e^{C_4 n \varepsilon_n^2 - (\alpha_n + \kappa_n)M\varepsilon_n^2} \iiint_{A_{n,M}} e^{\ell_n(T(\beta))} \Pi_0(d\theta, du, d\beta).$$

Now integrate out (θ, u) conditionally on β . Since the integrand depends on (θ, u) only through the indicator of $A_{n,M}$ and the prior,

$$N_n(A_{n,M}) \leq e^{C_4 n \varepsilon_n^2 - (\alpha_n + \kappa_n)M\varepsilon_n^2} \int e^{\ell_n(T(\beta))} m_n(\beta) \Pi_0^\beta(d\beta),$$

where $m_n(\beta) := \Pi_0(\{(\theta, u) : (\theta, u, \beta) \in A_{n,M}\} \mid \beta) \leq 1$. Hence

$$N_n(A_{n,M}) \leq e^{C_4 n \varepsilon_n^2 - (\alpha_n + \kappa_n)M\varepsilon_n^2} \int e^{\ell_n(T(\beta))} \Pi_0^\beta(d\beta).$$

Rewriting the last integral

$$N_n(A_{n,M}) \leq e^{\ell_n(\theta_0)} e^{C_4 n \varepsilon_n^2 - (\alpha_n + \kappa_n)M\varepsilon_n^2} \int e^{\ell_n(T(\beta)) - \ell_n(\theta_0)} \Pi_0^\beta(d\beta).$$

Since $E_{\theta_0} \left[\int e^{\ell_n(T(\beta)) - \ell_n(\theta_0)} \Pi_0^\beta(d\beta) \right] = \int E_{\theta_0} \left[\prod_{i=1}^n \frac{p_{T(\beta)}(Y_i)}{p_{\theta_0}(Y_i)} \right] \Pi_0^\beta(d\beta) = 1$. Hence, by Markov's inequality, for every fixed $C' > 0$, $P_{\theta_0}^n \left(\int e^{\ell_n(T(\beta)) - \ell_n(\theta_0)} \Pi_0^\beta(d\beta) > e^{C'n\varepsilon_n^2} \right) \leq e^{-C'n\varepsilon_n^2}$. Therefore, with high $P_{\theta_0}^n$ -probability, $N_n(A_{n,M}) \leq e^{\ell_n(\theta_0)} \exp\{(C_4 + C')n\varepsilon_n^2 - (\alpha_n + \kappa_n)M\varepsilon_n^2\}$.

3. Combining the numerator and denominator bounds. We now have, with high $P_{\theta_0}^n$ -probability,

$$\Pi_n(A_{n,M} \mid Y_{1:n}) \leq \exp\{(C_4 + C' + C)n\varepsilon_n^2 + \alpha_n C_2 \varepsilon_n^2 - (\alpha_n + \kappa_n)M\varepsilon_n^2\}.$$

Thus, if M is sufficiently large, by condition (v) $\liminf_{n \rightarrow \infty} (\alpha_n + \kappa_n) > 0$, then $\Pi_n(A_{n,M} \mid Y_{1:n}) \rightarrow 0$.

Since $\{G(\theta, u, \beta) > M\varepsilon_n^2\} \subseteq A_{n,M} \cup \mathcal{F}_n^c$, we have $\Pi_n(G(\theta, u, \beta) > M\varepsilon_n^2 \mid Y_{1:n}) \leq \Pi_n(A_{n,M} \mid Y_{1:n}) + \Pi_n(\mathcal{F}_n^c \mid Y_{1:n})$. The first term tends to zero by the preceding bound, while the second tends to zero by assumption (ii). Hence $\Pi_n(G(\theta, u, \beta) > M\varepsilon_n^2 \mid Y_{1:n}) \rightarrow 0$. \square

A.5 Proof of Theorem 5

Proof. Write

$$\Pi_n^{\text{rel},\beta}(d\beta | Y_{1:n}) = \frac{m_n^{\text{rel}}(\beta) \Pi_0^\beta(d\beta)}{\int m_n^{\text{rel}}(\beta) \Pi_0^\beta(d\beta)} \quad \text{and} \quad \Pi_n^{\text{ex},\beta}(d\beta | Y_{1:n}) = \frac{e^{\ell_n(T(\beta))} \Pi_0^\beta(d\beta)}{\int e^{\ell_n(T(\beta))} \Pi_0^\beta(d\beta)}.$$

On the set \mathcal{B}_n , the assumption implies

$$m_n^{\text{rel}}(\beta) = c_n e^{\ell_n(T(\beta))} \{1 + r_n(\beta)\}, \quad \sup_{\beta \in \mathcal{B}_n} |r_n(\beta)| \leq \delta_n,$$

with $P_{\theta_0}^n$ -probability tending to one. Since c_n does not depend on β , it cancels after normalization. Therefore, on \mathcal{B}_n , the two posterior densities differ only by $1 + r_n(\beta)$, uniformly convergent to one. Therefore,

$$\begin{aligned} & \|\Pi_n^{\text{rel},\beta}(\cdot | Y_{1:n}) - \Pi_n^{\text{ex},\beta}(\cdot | Y_{1:n})\|_{\text{TV}} \\ & \leq \|\Pi_n^{\text{rel},\beta}(\cdot \cap \mathcal{B}_n | Y_{1:n}) - \Pi_n^{\text{ex},\beta}(\cdot \cap \mathcal{B}_n | Y_{1:n})\|_{\text{TV}} + \Pi_n^{\text{rel},\beta}(\mathcal{B}_n^c | Y_{1:n}) + \Pi_n^{\text{ex},\beta}(\mathcal{B}_n^c | Y_{1:n}) \\ & \xrightarrow{P_{\theta_0}^n} 0. \end{aligned}$$

For the final claim, let $A_{n,M} := \{\beta : \rho(T(\beta), \theta_0) > M\varepsilon_n\}$. Then

$$|\Pi_n^{\text{rel},\beta}(A_{n,M} | Y_{1:n}) - \Pi_n^{\text{ex},\beta}(A_{n,M} | Y_{1:n})| \leq \|\Pi_n^{\text{rel},\beta}(\cdot | Y_{1:n}) - \Pi_n^{\text{ex},\beta}(\cdot | Y_{1:n})\|_{\text{TV}},$$

which converges to zero in $P_{\theta_0}^n$ -probability. Hence contraction rate of $T(\beta)$ under the exact projected posterior transfers to the relaxed posterior. \square

A.6 Sufficient conditions for the β -marginal convergence

We now proceed to give a set of sufficient conditions for the β -marginal convergence in Theorem 5. The content is that the relaxed inner integral over (θ, u) admits a local Laplace approximation around the zero-gap point $(T(\beta), u^*(\beta))$.

Theorem 7. *Let*

$$J_n(\beta) = \iint \exp\{\ell_n(\theta) - \ell_n(T(\beta))\} \exp\{-\alpha_n G(\theta, u, \beta)\} d\theta du.$$

Suppose there exists a measurable set $\mathcal{B}_n \subseteq \mathbb{R}^p$ such that $\Pi_n^{\text{ex},\beta}(\mathcal{B}_n | Y_{1:n}) \xrightarrow{P_{\theta_0}^n} 1$, and the following conditions hold uniformly over $\beta \in \mathcal{B}_n$.

- (i) *There is a unique zero-gap point $z^*(\beta) = (T(\beta), u^*(\beta))$ with $G(z^*(\beta), \beta) = 0$.*
- (ii) *There exists a positive definite matrix H_β such that, for every fixed $M > 0$,*

$$\sup_{\|h\| \leq M/\sqrt{\alpha_n}} \left| G(z^*(\beta) + h, \beta) - \frac{1}{2} h^\top H_\beta h \right| = o(\alpha_n^{-1}).$$

- (iii) *The Hessians are uniformly nondegenerate and asymptotically constant: $0 < \lambda_{\min} \leq \lambda_{\min}(H_\beta) \leq \lambda_{\max}(H_\beta) \leq \lambda_{\max} < \infty$, and there exists a deterministic sequence $d_n > 0$ such that $\det(H_\beta)^{-1/2} = d_n \{1 + o(1)\}$.*

(iv) For every fixed $M > 0$,

$$\sup_{\beta \in \mathcal{B}_n} \sup_{\|\theta - T(\beta)\| \leq M/\sqrt{\alpha_n}} |\ell_n(\theta) - \ell_n(T(\beta))| \xrightarrow{P_{\theta_0}^n} 0.$$

(v) There exists $c_0 > 0$ such that, for all sufficiently large n ,

$$G(z^*(\beta) + h, \beta) \geq c_0 \|h\|^2$$

whenever $\|h\|$ is sufficiently small, uniformly in $\beta \in \mathcal{B}_n$. Moreover, for every $\eta > 0$,

$$\lim_{M \rightarrow \infty} \limsup_{n \rightarrow \infty} P_{\theta_0}^n \left(\sup_{\beta \in \mathcal{B}_n} \alpha_n^{m/2} J_{n,2}(\beta; M) \geq \eta \right) = 0,$$

with $J_{n,2}(\beta; M)$ a tail integral defined as in the proof.

Then there exists a deterministic sequence $c_n = (2\pi)^{m/2} \alpha_n^{-m/2} d_n$ such that

$$\sup_{\beta \in \mathcal{B}_n} \left| \frac{J_n(\beta)}{c_n} - 1 \right| \xrightarrow{P_{\theta_0}^n} 0 \Leftrightarrow \sup_{\beta \in \mathcal{B}_n} \left| \frac{m_n^{\text{rel}}(\beta)}{c_n e^{\ell_n(T(\beta))}} - 1 \right| \xrightarrow{P_{\theta_0}^n} 0.$$

Proof. Fix $\beta \in \mathcal{B}_n$, and write $z = (\theta, u)$, $z^* = z^*(\beta) = (T(\beta), u^*(\beta))$. Then $J_n(\beta) = \int \exp\{\ell_n(\theta) - \ell_n(T(\beta))\} e^{-\alpha_n G(z, \beta)} dz$.

Make the change of variable $h = z - z^*$. Then

$$\begin{aligned} J_n(\beta) &= \int \exp\{\ell_n(T(\beta) + h_\theta) - \ell_n(T(\beta))\} e^{-\alpha_n G(z^* + h, \beta)} dh, \\ &= \underbrace{\int_{\|h\| \leq M/\sqrt{\alpha_n}} \exp\{\ell_n(T(\beta) + h_\theta) - \ell_n(T(\beta))\} e^{-\alpha_n G(z^* + h, \beta)} dh}_{J_{n,1}(\beta; M)} \\ &\quad + \underbrace{\int_{\|h\| > M/\sqrt{\alpha_n}} \exp\{\ell_n(T(\beta) + h_\theta) - \ell_n(T(\beta))\} e^{-\alpha_n G(z^* + h, \beta)} dh}_{J_{n,2}(\beta; M)}. \end{aligned}$$

where h_θ denotes the θ -component of h .

Fix $\eta > 0$. By assumption (v), there exists $M < \infty$ sufficiently large such that

$$\sup_{\beta \in \mathcal{B}_n} J_{n,2}(\beta; M) \leq \eta \alpha_n^{-m/2}$$

with $P_{\theta_0}^n$ -probability tending to one. For this fixed M , it remains to approximate $J_{n,1}(\beta; M)$.

On the set $\|h\| \leq M/\sqrt{\alpha_n}$, assumption (iv) implies

$$\sup_{\beta \in \mathcal{B}_n} \sup_{\|h\| \leq M/\sqrt{\alpha_n}} |\exp\{\ell_n(T(\beta) + h_\theta) - \ell_n(T(\beta))\} - 1| \rightarrow 0$$

in $P_{\theta_0}^n$ -probability. Also, by assumption (ii),

$$\sup_{\beta \in \mathcal{B}_n} \sup_{\|h\| \leq M/\sqrt{\alpha_n}} \left| \alpha_n G(z^*(\beta) + h, \beta) - \frac{1}{2} (\sqrt{\alpha_n} h)^\top H_\beta (\sqrt{\alpha_n} h) \right| \rightarrow 0$$

as $n \rightarrow \infty$. Therefore,

$$\sup_{\beta \in \mathcal{B}_n} \left| J_{n,1}(\beta; M) - \int_{\|h\| \leq M/\sqrt{\alpha_n}} \exp\left\{ -\frac{\alpha_n}{2} h^\top H_\beta h \right\} dh \right| = o_{P_{\theta_0}^n}(\alpha_n^{-m/2}).$$

Now set $t = \sqrt{\alpha_n} h$. Then

$$\sup_{\beta \in \mathcal{B}_n} \left| J_{n,1}(\beta; M) - \alpha_n^{-m/2} \int_{\|t\| \leq M} \exp\left\{-\frac{1}{2} t^\top H_\beta t\right\} dt \right| = o_{P_{\theta_0}^n}(\alpha_n^{-m/2}).$$

uniformly over $\beta \in \mathcal{B}_n$.

Combining this with the tail bound gives

$$\sup_{\beta \in \mathcal{B}_n} \left| J_n(\beta) - \alpha_n^{-m/2} \int_{\|t\| \leq M} \exp\left\{-\frac{1}{2} t^\top H_\beta t\right\} dt \right| \leq \eta \alpha_n^{-m/2} + o_{P_{\theta_0}^n}(\alpha_n^{-m/2}).$$

Since $\eta > 0$ was arbitrary, letting $M \rightarrow \infty$ in the Gaussian integral and using assumption (iii), we conclude that

$$J_n(\beta) = \alpha_n^{-m/2} (2\pi)^{m/2} \det(H_\beta)^{-1/2} \{1 + o_{P_{\theta_0}^n}(1)\}$$

uniformly over $\beta \in \mathcal{B}_n$.

Finally, since $\det(H_\beta)^{-1/2} = d_n \{1 + o(1)\}$ uniformly over $\beta \in \mathcal{B}_n$, it follows that

$$J_n(\beta) = (2\pi)^{m/2} \alpha_n^{-m/2} d_n \{1 + o_{P_{\theta_0}^n}(1)\}$$

uniformly over $\beta \in \mathcal{B}_n$. This proves the claim. \square

Remark 3. In the above result, the regime $\alpha_n \rightarrow \infty$ is used to induce localization of the relaxed inner integral on the scale $\alpha_n^{-1/2}$ around the zero-gap point $(T(\beta), u^*(\beta))$. In principle, the approximation $\sup_{\beta \in \mathcal{B}_n} \left| \frac{m_n^{\text{rel}}(\beta)}{c_n e^{\ell_n(T(\beta))}} - 1 \right| \xrightarrow{P_{\theta_0}^n} 0$ may still hold without requiring $\alpha_n \rightarrow \infty$, but we conjecture that it may hold under different conditions ensuring that the relaxed inner integral is already concentrated near $(T(\beta), u^*(\beta))$ at a fixed scale and that the likelihood is sufficiently flat on that scale. We leave this as a potential future work.

A.7 Proof of Theorem 6

Proof. By Theorem 4, the posterior duality gap is of order ε_n^2 , and therefore Theorem 1 implies that

$$\|\theta - T(\beta)\|_2 = O_{P_{\theta_0}^n}(\varepsilon_n)$$

under the relaxed posterior. By Theorem 5, contraction of $T(\beta)$ under the exact projected posterior transfers to the relaxed posterior, so

$$\Pi_n^{\text{rel}, \beta}(\rho(T(\beta), \theta_0) > M\varepsilon_n \mid Y_{1:n}) \xrightarrow{P_{\theta_0}^n} 0$$

for every sufficiently large $M > 0$. The conclusion then follows from

$$\rho(\theta, \theta_0) \leq C \|\theta - T(\beta)\|_2 + \rho(T(\beta), \theta_0).$$

\square

B Additional results from data application

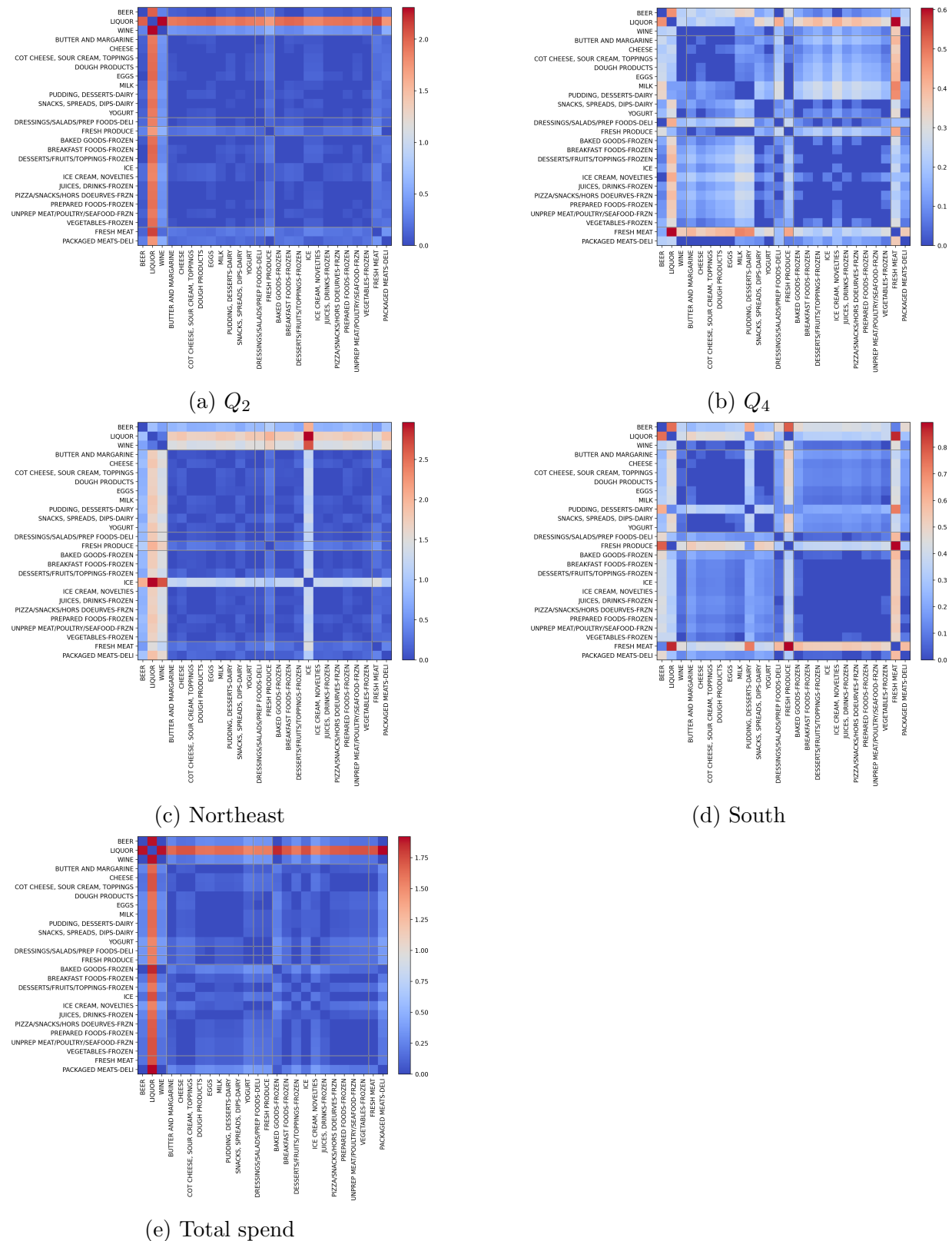


Figure 7: Absolute pairwise posterior mean differences under the gap-shrinkage model, ordered by department.